Exosomes derived from miR-301a-3p-overexpressed adipose-derived mesenchymal stem cells reverse hypoxia-induced erectile dysfunction in rat models

Li Liang
Shanghai Jiao Tong University School of Medicine
Dachao Zheng
Shanghai Jiao Tong University School of Medicine
Chao Lu
Shanghai Jiao Tong University School of Medicine
Qinghong Xi
Shanghai Jiao Tong University School of Medicine
Hua Bao
Shanghai Jiao Tong University School of Medicine
Wengfeng Li
Shanghai Jiao Tong University School of Medicine
Yufei Gu
Shanghai Jiao Tong University School of Medicine
Yuanshen Mao
Shanghai Jiao Tong University School of Medicine
Bin Xu
Shanghai Jiao Tong University School of Medicine
Xin Gu (guyiran08612@163.com)
Shanghai Jiao Tong University School of Medicine https://orcid.org/0000-0001-5328-3719

Research

Keywords: erectile dysfunction, chronic intermittent hypoxia, exosomes, miR-301a-3p, autophagy

Posted Date: December 5th, 2020

DOI: https://doi.org/10.21203/rs.3.rs-51339/v2

Version of Record: A version of this preprint was published on January 25th, 2021. See the published version at https://doi.org/10.1186/s13287-021-02161-8.

Abstract

Background: Erectile dysfunction (ED) has often been observed in patients with obstructive sleep apnea (OSA). Research on adipose-derived mesenchymal stem cells (ADSCs)-derived exosomes has shown that they have significant therapeutic effects in many diseases including ED.

Methods: In this study, ED was induced in Sprague Dawley (SD) rats using chronic intermittent hypoxia (CIH) exposure. CIH-mediated influences were then measured in the corpus cavernous smooth muscle cells (CCSMCs).

Results: Our data showed that miR-301a-3p-enriched exosomes treatment significantly recovered erectile function in rats and CCSMCs by promoting autophagy and inhibiting apoptosis. The treatment also significantly recovered the level of alpha Smooth Muscle Actin (α-SMA) in rats and CCSMCs. Bioinformatics predicted that Phosphatase and tensin homolog (PTEN) and Toll-like receptor 4 (TLR4) might be targets of miR-301a-3p.

Conclusions: Our results indicate that PTEN-overexpression vectors or TLR4-overexpression vectors reverse the therapeutic effects achieved by miR-301a-3p in CCSMCs indicating that PTEN/HIF-1α and TLR4 signaling pathways play key roles in the progression of ED. The findings in this study suggest that miR-301a-3p should be considered as a new therapeutic target for treating ED associated with OSA.

1. Introduction

Erectile dysfunction (ED), also known as inadequate penile erection, is a common clinical entity that mainly affects males older than 40 years[1]. It is defined as the inability to achieve and maintain an adequate erection to permit satisfactory sexual intercourse[2] resulting in dissatisfaction with sex life in a significant proportion of men [3]. Several factors are associated with ED including smoking, hormonal imbalance, general health status of the individual, diabetes mellitus, cardiovascular diseases and psychiatric disorders[4]. In addition, ED is the most common long-term side effect of active therapy for early prostate cancer treatment including robotic-assisted laparoscopic radical prostatectomy (RALP) [5, 6]. Despite the use of nerve-sparing techniques, as high as 90% rates of post-RALP ED have been reported mainly due to periprostatic and cavernous nerve (CN) damage [7].

Chronic intermittent hypoxia (CIH) is one of the most important and direct consequences of obstructive sleep apnea (OSA)[8, 9] with studies showing a higher ED incidence in male patients with chronic hypoxia[10]. Hypoxia may affect erectile function, neuronal nitric oxide synthase (nNOS) and endothelial nitric oxide synthase (eNOS) expression leading to erectile dysfunction under hypoxic conditions in murine models[11, 12]. Constitutively expressed nNOS and eNOS isoforms mediate penile erection by producing nitric oxide (NO), which has been recognized as playing a major role in the physiology of penile erection[1, 2]. Catalyzed by NOS and produced from L-Arginine, NO activates guanylate cyclase (GC)

which converts guanosine triphosphate (GTP) to cyclic guanosine monophosphate (cGMP) leading to relaxation of vascular smooth muscles and vasodilation[13]. Oral phosphodiesterase type 5 (PDE-5) inhibitors were the first and most effective form of oral therapies recommended for the treatment of ED [13]. However, potential side effects such as anterior ischemic optic neuropathy and increased risk of stroke have hindered the use of PDE-5 inhibitor[14].

Recent studies have shown that adipose-derived stem cells (ADSCs) therapy has therapeutic effects for ED resulting from cavernous nerve injury[15, 16]. Exosomes are membrane vesicles that are secreted by most cells. Exosomes having a diameter of 30-100 nm contain many macromolecular components including proteins, mRNAs, and microRNAs (miRNAs) which can regulate intracellular signaling pathways[17].Several studies have shown that ADSC-derived exosomes play an important role in ADSC therapy where the use of exosomes from miRNA-modified ADSC to deliver exogenous miRNAs provides protection from various diseases[18-21]. Studies have found that exosomes derived from ADSCs and mesenchymal stem cells (MSCs) exert therapeutic effect on ED in rat models having diabetes and cavernous nerves injury[22-25]. However, there is no report on the treatment of ED by exogenous miRNA-modified ADSC-derived exosomes. Therefore, the study of miRNA-overexpressed ADSC-derived exosomes treatment for ED is vital. Previous studies have shown that miR-301a-3p is a key factor in pancreatic cancer, breast cancer, carcinoma and schizophrenia[26-29]. One study indicated that the level of miR-301a-3p in the corpus cavernosum of type 2 diabetes mellitus-associated erectile dysfunction (T2DMED) mice was significantly decreased compared with normal mice[30]. In addition, our preliminary research found that miR-301a-3p was significantly down-regulated in ED patients and rats with CIH-induced ED. This led to our focus on the potential role of miR-301a-3p in the progression of ED.

In this study, we used exosomes derived from miR-301-3p-overexpressed ADSC as the therapeutic medium. We analyzed intracavernous pressure (ICP) and arterial pressure (AP) in rat models after CIH exposure. Expression levels of nNOS and eNOS were measured to investigate the potential effects of miR-301a-3p-enriched exosomes treatment. Analysis of the expression levels of apoptosis, autophagosomes, autolysosomes and other indicators associated with ED was done using CIH exposed murine models. Results showed that miR-301a-3p-enriched exosomes treatment had significant therapeutic effects on rats after CIH exposure. Further study of signaling pathways indicated that phosphatase and tensin homolog (PTEN) and Toll-like receptor 4 (TLR4) might be directly targeted by miR-301a-3p with overexpression of both reversing protection effects induced by miR-301a-3p. Our findings indicate that miR-301a-3p should be considered as a new therapeutic target in treating ED patients.

2. Materials And Methods

2.1Animals

Sprague Dawley (SD) rats (male, weight 180-220 g) were purchased from Shanghai SLAC Laboratory Animal Co., Ltd. Animals were maintained under controlled conditions with a 12/12 hours light/dark photoperiod, temperature of 22±3°C and humidity of 60±5%. This study was conducted with strict accordance to the Guide for the Care and Use of Laboratory Animals (Eighth Edition, 2011, published by The National Academies Press, 2101 Constitution Ave. NW, Washington, DC 20055, USA). The protocol was reviewed and approved by the Shanghai Ninth People's Hospital Institutional Review Board (Permit Number: HKDL2013001b). Surgery was performed under sodium pentobarbital anesthesia with all efforts being made to minimize suffering.

2.2 Patient samples

A sample size of 30 OSA patients with ED admitted at Shanghai Ninth People's Hospital, Shanghai, China was enrolled. According to hospital records, the patients had been clinically diagnosed with ED. The age of the patients ranged from 30 to 65 years. Patients with hypertension, diabetes, trauma and surgery history were excluded. Thirty healthy people to be used as controls were also recruited from the hospital. Serum samples were taken within 24 hours of symptom onset and frozen in liquid nitrogen. Ethical approval for the study was provided by the Independent Ethics Committee of Shanghai Ninth People's Hospital, Shanghai, China. Guidelines from the Ethics Committee were followed where informed and written consent was obtained from all patients or their advisors before samples were collected.

2.3 Culturing ADSCs

Adipose tissues collected from SD rats were washed with pre-cooled phosphate-buffered saline (PBS) and cut into 1mm^2 pieces. Tissues were digested using collagenase followed by centrifugation at 4000×g for 5 minutes. Obtained cell pellet was then suspended in Dulbecco's modified Eagle's medium (DMEM) containing 10% fetal bovine serum (FBS), 1% penicillin-streptomycin and 2 mmol/L L-glutamine. The cells were then cultured in a controlled environment having 5% CO2 and a temperature of 38°C for 48 hours. Cells were then transferred into fresh culture medium with subsequent subculture every 3 days. When cells were approximately 90% confluent, they were passaged and used at passage three. For Immunofluorescence: Cells were then incubated with conjugated monoclonal antibodies against CD29 (ab179471, 1:200), CD44 (ab189524, 1:200), CD90 (ab225, 1:200), CD105 (ab2529, 1:200) and vWF (ab194405, 1:200) all from Abcam to confirm the identity of ADSCs. Isotype-identical antibodies (#550343, 1:200, PharMingen, San Diego, CA, USA) were used as controls. For Flow cytometer: Cells were identified and selected by flow cytometry (FCM) with anti-CD29, CD44, CD90, and CD105 (1:200; Abcam Inc.). After being subcultured to the third generation, cells at 80% confluence were washed twice with PBS followed by digestion with 0.25% trypsin–EDTA (ThermoFisher Scientific, USA). The cells were then centrifuged at 1000 rpm and washed with PBS. After incubation with antibodies and their isotype

controls (1:200) (PharMingen) at 4 °C for 30 min, the cells were flowed through the cytometer at about 1000 cells per second and analysis.

2.4 Isolation of exosomes

Adipose-derived stromal cells collected from miR-301a-3p overexpression, control and NC groups at 80%-90% confluence were washed with PBS and cultured in microvascular endothelial cell growth medium-2 media deprived of FBS. ADSCs were then supplemented using 1×serum replacement solution (PeproTech) for 24 hours. Dead cells and debris were removed by centrifugation of ADSCs at 300×g for 10 minutes and 2000×g for 10 minutes followed by mixing 10 mL of the supernatant with 5 mL of ExoQuick-TC reagent (System Biosciences). The mixture was then centrifuged at 1500×g for 30 minutes, with the resulting exosome-containing pellet being re-suspended in nuclease-free water. TRIzol-LS (Invitrogen) and Exosomal Protein Extraction (Invitrogen) kits were used for extracting total RNA and protein, respectively. Isolated exosomes were used immediately for experiments or stored at -180°C. Sizes of purified exosomes were determined using a NanoSight LM10 (Malvern Instruments) nanoparticle tracking system.

2.5 CIH exposure-induced ED rat model

Twenty-four male SD rats were randomly divided into control, CIH, CIH + exosomes from untreated ADSCs (Exo) and CIH + miR-301a-3p-enriched exosomes (Exo-301a) groups (n = 6). An oxygen sensor was placed at the bottom of the chamber to measure the oxygen content in the CIH exposure chamber over the course of several cycles. Animals were exposed to 2 minutes of 5% O_2 for each 4-minute cycle with each challenge lasting 8 hours. The challenge was done for eight weeks during the daytime from 8am to 4pm. Sham group rats were exposed to 21% O_2. Exosomes (400 μg of protein) were isolated using 200 μL PBS and then administered using intracavernous injection for Exo groups, whereas control rats received an equal volume of PBS. Exosomes were administered to the rats every week for eight weeks.

2.6 Erectile function Measurement

After eight weeks of CIH exposure, intracavernous pressure (ICP) and Mean carotid artery pressure (MAP) were measured to evaluate erectile function as described in our previous article[7]. Penile tissues were then harvested, under euthanasia, for further histological studies.

2.7 Immunofluorescence

Harvested tissues were immersed in optimal cutting temperature compound and immediately frozen in liquid nitrogen. The tissues were cut into sections having a thickness of 5μm followed by immunofluorescence staining as described in[31]. Primary antibodies used in this study were eNOS (ab76198), nNOS (ab76067) and Phalloidin (ab176753) all obtained from Abcam. Secondary antibodies included Alexa-488, Texas Red-conjugated antibodies, (1:500; Invitrogen, Carlsbad, CA, USA) and Texas Red goat anti-rabbit IgG (1:200; Life Technologies, Grand Island, NY, USA). Nuclei were stained using DAPI (1:10,000, Invitrogen, Carlsbad, CA, USA). The number of cells in each image was counted with DAPI cells and positive cells. Ratio of positive nNOS counts to DAPI were used to analyze the nerve fibers in the dorsal section of the penis. Smooth muscle and endothelial stains were analyzed using the ratio of positively stained areas of phalloidin and eNOS to DAPI in the corpora cavernosa.

2.8 CCSMCs culture and CIH exposure

Rats were sacrificed where on a sterile table, the penis was excised and placed in a sterile Petri dish followed by two washes using PBS. The skin around the penis was carefully peeled away, along with the albuginea, urethral sponge, cavernous body, and other vessels. The corpus cavernosum was cut into $1mm^3$ tissue blocks that were placed in a cell culture flask containing 0.5% type I collagenase solution (Sigma). Cells were cultured at 37°C with shaking in a humidified atmosphere having 95% air and 5% CO_2 for 3 hours. The cells were then filtered and centrifuged followed by the addition of 3ml F12 medium (Invitrogen) containing 20% fetal bovine serum (Invitrogen) and incubated at 37°C and 5% CO_2. Long, spindle-shaped SMCs were observed at the bottom of the $25cm^2$ culture flasks after incubating for 24 hours. For CIH exposure, CCSMCs were exposed to 5min of 14% to 15% O_2 during each 60min cycle for 24 hours by using BioSpherix-OxyCycler C42system (BioSpherix, Redfield, NY). All cells were cultured for 24 hours followed by co-culturing with miR-301a-3p-enriched exosomes for 48 hours.

2.9 Statistical analysis

Results are expressed as the mean ± SD. All the data obtained from this study was analyzed using GraphPad 9.0. Two groups analysis was performed t-test (two tailed). One-way ANOVA was used among various groups with $p < 0.05$ being considered as statistically significant.

More detailed materials and methods are in the Supplementary Methods.

3. Results

3.1 CIH exposure significantly down-regulates miR-301a-3p in patients with ED and in rats induced with ED

ADSCs obtained from adipose tissues of SD rats displayed a typical fibroblastic-like morphology under the microscope (Fig. 1A). Oil Red O staining confirmed that they were undergoing adipogenesis (Fig. 1B). To confirm the identity of ADSCs, they were incubated with conjugated monoclonal antibodies against CD29, CD44, CD90, CD105, CD34 and vWF with isotype-identical antibodies (PharMingen) being used as controls. Immunofluorescence and flow cytometer results showed that ADSCs were positive for the mesenchymal stem cell (MSC) markers CD29, CD34, CD44, CD90 and CD 105 (Fig. 1C and D). The sequences between hsa-miR-301a-3p (human) and rno-miR-301a-3p (rat) were same (obtained from http://www.mirbase.org/) (Fig. 1E) and RT-qPCR analysis of serum samples collected from 30 ED patients showed that expression levels of hsa-miR-301a-3p in ED patients were significantly lower than those in healthy patients (p<0.001) (Fig. 1F). To further determine the expression of rno-miR-301a-3p, CIH exposure was done on SD rats. Results showed that rno-miR-301a-3p expression was inhibited at gene level in CIH exposed rats compared to control group (n=8, p<0.01) (Fig. 1G).

ADSC-derived exosomes were isolated and confirmed under a microscope (Fig. 1H) with transmission electron microscope (TEM) analysis showing that the diameter of most exosomes was approximately 100mm (Fig. 1I). Examination of ADSCs and exosomes using Western blot resulted in exosomes testing positive against exosome markers TSG101, CD9 and CD63 while ADSCs tested negative (Fig. 1J). After transfection with miR-301a-3p-overexpressed mimic, ADSCs and ADSC-derived exosomes were analyzed using RT-qPCR. Results confirmed the overexpression of miR-301a-3p in both ADSCs and ADSC-derived exosomes, compared to control and negative control groups (Fig. 1J). The results indicated that miR-301a-3p was significantly down-regulated in ED patients and CIH exposure rats. In addition, miR-301a-3p mimic had a good transcription efficiency in ADSCs.

3.2 CIH exposure negatively influences erectile function while miR-301a-3p-enriched exosomes treatment repairs the damage in SD rats

Masson trichrome staining of actin and collagen was done for each group where smooth muscle and connective tissue in the corpus cavernosum stained red and blue, respectively. Results indicated a decrease in the proportion of smooth muscle when CIH exposure rats were compared with the sham group after (p<0.001). When compared with CIH exposure group, miR-301a-3p-enriched exosomes treatment significantly promoted the proportion of smooth muscle indicating that exosomes treatment had therapeutic effects on the repair of smooth muscle (p<0.001) (Fig. 2A and B). Results obtained after Phalloidin staining indicated that CIH exposure destroyed F-actin. Significantly more stained cytoskeleton area was observed after normal exosomes treatment and miR-301a-3p-enriched exosomes treatment with the effects of the latter being more pronounced (Fig. 2C and D).

The ratio of ICP/RT-AP was used to assess erectile function (Fig. 2E) with results showing that CIH exposure significantly inhibited erectile function in SD rats (Fig. 2G). Normal exosomes and miR-301a-3p-enriched exosomes treatments had significant effects on recover ICP/RT-AP when compared to CIH exposure group (p<0.001) with miR-301a-3p-enriched exosomes having more pronounced effects (Fig. 2G). Western blot analysis was done to measure the level of myofibroblast formation with results indicating that α-SMA was down-regulated after CIH exposure. However, exosome treatment significantly increased the expression of α-SMA when compared with CIH exposure group (Fig. 2F).

To determine the level of nNOS in DNP of the penis, harvested tissues were prepared for immunofluorescence staining and Western blot analysis. Results showed no significant changes in the ratio of nNOS-positive nerve counts/DAPI in all areas of CIH exposure groups when compared with Sham groups indicating that CIH exposure did not alter NO release from peripheral nerve endings (Fig.3 A-C). This was confirmed by the results of Western blot analysis which indicated that CIH exposure had no effect on the expression of nNOS. Interestingly, CIH exposure stimulated the expression of iNOS while miR-301a-3p-enriched exosomes reduced its expression (Fig. 3D and E). Immunofluorescence staining of endothelial cells showed that eNOS expression decreased significantly after CIH exposure (p<0.00) when compared to Sham group. Exosomes treatment had positive effects on recovering the expression level of eNOS with miR-301a-3p-enriched exosomes treatment having significantly better results (Fig. 3F-H). Results indicate that CIH exposure negatively affected erectile function while miR-301a-3p-enriched exosomes treatment had significant remediation effects on SD rats, including ICP/RT-AP and expression levels of α-SMA and eNOS.

3.3 miR-301a-3p suppressed the level of PTEN and TLR4 *in vivo*

DNP tissue were collected from SD rats in all groups (Sham, CIH, CIH+EXO, CIH+EXO-301a) and analyzed using RT-qPCR to determine the signaling pathway used by miR-301a-3p to influence erectile function. RT-qPCR results showed that the expression level of miR-301a-3p in rat DNP tissue significantly decreased in CIH exposure group when compared to Sham group (p<0.001). There was no significant difference between CIH exposure group and CIH+EXO group, while miR-301a-3p was significantly overexpressed in CIH+EXO-301a group (Fig. 4A). Furthermore, the results showed a significant increase of PTEN and TLR4 gene levels in CIH and CIH+EXO groups (Fig. 4B and D). Treatment with miR-301a-3p reversed the expression of PTEN and TLR4 leading to a decrease in PTEN and TLR4 levels (Fig. 4B and D). Protein levels of PTEN and TLR4 in rat DNP tissue in each group were confirmed using Western blot analysis (Fig. 4C and E).

Results obtained after Western blot analysis in rat DNP tissue showed that CIH exposure directly induced overexpression of LC3I/II and p65 in the nucleus (Fig. 4C and E) indicating that the level of autophagy was up-regulated by CIH exposure. Up-regulated autophagy was also confirmed by the inhibited expression of p62 (Fig. 4C). Exosomes treatment increased the level of autophagy through overexpressing LC3I/II and p65 while the levels of p62 decreased with miR-301a-3p enriched exosomes having a more pronounced effect (Fig. 4C and E). These results suggest that PTEN and TLR4 can be directly targeted by miR-301a-3p.

Bioinformatics was used to predict the possible targets in the determination of the potential association between miR-301a-3p and PTEN/TLR4 with results showing that both PTEN and TLR4 could be possible targets of miR-301a-3p (Fig. 5A and C). Dual-luciferase reporter assay results showed that overexpression of miR-301a-3p reduced the intensity of fluorescence in CCSMCs transfected with TLR4-WT and PTEN-WT vectors while having no effect on CCSMCs transfected with TLR4-MUT and PTEN-MUT vectors (Fig. 5B and D). RT-qPCR and Western blot results further confirmed that both TLR4 and PTEN were inhibited at mRNA and protein level after cells were transfected with miR-301a-3p (Fig. 5E and F). Combining both sets of results made a clear indication that both PTEN and TLR4 are direct targets of miR-301a-3p.

3.4 miR-301a-3p-enriched exosomes inhibits CIH-induced apoptosis and up-regulates CIH-induced overexpression of autophagy in CCSMCs

For CIH exposure, CCSMCs were exposed to 5 s of 14% to 15% O_2 during every 60 s cycle for 24 h. All cells were cultured for 24h and Co-culturing with miR-301a-3p-enriched exosomes for 48 h. Results obtained after CIH exposure of CCSMCs indicated that α-SMA was down-regulated at protein level. On the other hand, exosome treatment increased the level of α-SMA after CIH exposure with miR-301a-3p-enriched exosomes treatment having a more significant effect than normal exosomes treatment (Fig. 6A). Flow cytometry with Annexin V- FITC staining was used to assess the apoptosis rate with results showing that CIH exposure directly led to a significant increase in the apoptosis rate. However, exosomes treatment inhibited apoptosis with miR-301a-3p-enriched exosomes treatment having a significantly higher CIH-induced apoptosis rate inhibition than normal exosomes treatment (p<0.001) (Fig. 6 B and C). Levels of miR-301a-3p, PTEN, and TLR4 were analyzed using RT-qPCR. As we had hypothesized, results indicated that miR-301a-3p levels decreased after CIH exposure (p<0.01) when compared to control group. There was no significant difference between CIH group and CIH+EXO group (Fig. 6D). However, miR-301a-3p-enriched exosomes treatment led to a significant overexpression of miR-301a-3p levels in CCSMCS after CIH exposure (Fig. 6D). Both PTEN and TLR4 levels increased significantly after CIH exposure while miR-301a-3p-enriched exosomes treatment significantly decreased the mRNA expression level of PTEN and TLR4 (Fig. 6D). Results obtained after Western blot analysis confirmed the expression levels of PTEN and TLR4 (Fig. 6G and H).

In addition, Western blot results showed that CIH exposure directly induced overexpression of LC3I/II and p65 in the nucleus indicating that the level of autophagy was up-regulated by CIH exposure (Fig. 5G and H). Increased autophagy was confirmed by the inhibited expression of p62 (Fig. 5G). The level of autophagy was further increased by exosomes treatment, especially treatment with miR-301a-3p-enriched exosomes (Fig. 5G and H). Autophagic flux analysis was further done where CCSMCs were transfected with mRFP-GFP-LC3 with results showing that the quantity of autophagosomes, autolysosomes, and autophagic vacuoles increased significantly after CIH exposure (Fig. 5 I-L). There was no significant difference between CIH group and CIH+EXO group, while miR-301a-3p led to a significant increase of autophagosomes, autolysosomes, and autophagic vacuoles in CCSMCs ((Fig. 5 I-L)). Our findings suggest that miR-301a-3p-enriched exosomes treatment inhibits CIH-induced apoptosis and up-regulates CIH-induced overexpression of autophagy in CCSMCs.

3.5 PTEN or TLR4 overexpression significantly suppresses exo-301a-3p-induced positive effect on autophagy and inhibitory effect on apoptosis

PTEN-overexpression (PTEN-OE) and TLR4-overexpression (TLR4-OE) vectors were constructed to determine whether miR-301a-3p/PTEN/TLR4 signaling pathways were involved in the progression of apoptosis and autophagy. After transfection, overexpression of PTEN was detected using RT-qPCR and Western blot analysis (Fig. 7A and B). Western blot results confirmed that miR-301a-3p reversed the CIH-induced suppressive effects on α-SMA while PTEN-OE inhibited the expression level of α-SMA in CIH+EXO-301a+PTEN-OE group (Fig. 7C). On the other hand, miR-301a-3p-enriched exosomes treatment resulted in CIH-induced increase of HIF-1α and LC3I/II levels while at the same time inhibiting the expression of p62 (Fig. 7G). All miR-301a-3p-induced effects on levels of HIF-1α, LC3I/II, and p62 were reversed by PTEN-OE (Fig. 7G). Flow cytometry results indicated that CIH exposure led to a significantly high apoptosis rate with the effects promoting apoptosis being suppressed by miR-301a-3p. However, PTEN-OE reversed the miR-301a-3p-induced inhibitory effects on apoptosis (Fig. 7D and E). In addition, autophagic flux analysis confirmed that CIH-induced increase of autophagosomes, autolysosomes, and autophagic vacuoles after miR-301a-3p-enriched exosomes treatment (Fig. 7H-K). However, transfection with PTEN-OE significantly decreased the quantity of autolysosomes, and autophagic vacuoles in CCSMCs.

Potential roles of TLR4 were also determined where the effectiveness of TLR4-OE was checked at protein and gene level (Fig. 7L and M). Flow cytometry results showed that the high CIH-induced apoptosis rate was inhibited by miR-301a-3p. TLR4-OE significantly suppressed miR-301a-induced inhibitory effects thereby promoting increased apoptosis (Fig. 7N and O). Similar to results of CIH+EXO-301a+PTEN-OE group, miR-301a-induced expression of high α-SMA levels was significantly suppressed by TLR4-OE

vectors (Fig. 7P). In addition, Western blot analysis confirmed that TLR4-OE reversed the miR-301a-3p-inhibted expression level of p62 in CCSMCs (Fig. 7Q and R). When combined, the results suggest that both PTEN-OE and TLR4-OE significantly suppressed miR-301a-3p-induced positive effects on autophagy and inhibitory effects on apoptosis.

4. Discussion

There is an increase in the incidences of prostate cancer in line with increasing male life expectancy. Despite the use of nerve-sparing techniques during the treatment of prostate cancer, rates as high as 90% of post-RALP ED have been reported[7]. Other important risk factors associated with ED are CIH and sleep apnea problems in men [32]. Traditionally, clinical interventions have been limited to managing the chronic form of ED using phosphodiesterase-5 inhibitors, intracavernosal injections, vacuum devices, and penile prostheses. Recently, exosomes have been found to have therapeutic effects on ED in rat models having diabetes and cavernous nerves injury [22, 24, 25]. In this study, we designed experiments to investigate the effects of CIH exposure in rat models and CCSMCs. The main aim of the study was to determine the role that miR-301a-3p plays in CIH exposure rats and CCSMCs as well as determining its molecular mechanisms.

In the treatment of ED, cavernous smooth muscle plays a key role in recovery of erectile function [33]. Our results indicated that miR-301a-3p-enriched exosomes treatment significantly increased the proportion of smooth muscle in CIH exposure rats. Moreover, miR-301a-3p-enriched exosomes led to a significantly raised expression of α-SMA. Erectile function recovery was also determined by measuring ICP and RT-AP levels. Generally, both exosome treatments had significant effects on recover ICP/RT-AP in CIH exposure rats with miR-301a-3p-enriched exosomes treatment having better therapeutic effects. Production of NO, a key factor in erectile function, was determined by examining the levels of nNOS and eNOS. Results showed that the expression level of eNOS in DNP and sinusoid decreased significantly in CIH exposure groups when compared with Sham groups. On the other hand, miR-301a-3p-enriched exosomes treatment led to a significantly higher expression of eNOS in CIH exposure rats. Results from this study indicated that miR-301a-3p-enriched exosomes has therapeutic effects on recovering erectile function damaged after CIH exposure.

A previous study recommends using MSC-induced promotion of autophagy to treat ED [34]. In this study, we examined the expression levels of LC3I/II, p62 and p65. Results showed that autophagy was stimulated to a higher level in CIH exposure rats and CCSMCs. miR-301a-3p-enriched exosomes treatment increased the number of autophagosomes, autolysosomes, and autophagic vacuoles in rats and CCSMCs after CIH exposure. The level of apoptosis was assessed using flow cytometry after Annexin V-FITC staining. We found that CIH exposure increased the apoptosis rate in CCSMCs, while miR-301a-3p reversed these effects by decreasing the apoptosis rate. Our findings supported the prediction by

bioinformatics that PTEN and TLR4 could be targets of miR-301-3p. Therapeutic effects of miR-301a-3p-enriched exosomes treatment on the levels of HIF-1α, α-SMA, autophagy and apoptosis were reversed by both PTEN-OE and TLR4-OE. These findings suggest that miR-301-3p directly targets PTEN and TLR4 in the regulation of erectile function. However, there is need to further investigate miR-301a-3p, PTEN and TLR4 as possible therapeutic targets for treating ED. In this study, performing CIH-induced injury in cell experiments enabled the measurement of ICP/RT-AP and smooth muscle staining in SD rats. Due to a number of factors, like the function of PTEN-OE and TLR4-OE not being studied in SD rats, this study still needs further development.

5. Conclusions

In summary, we found that miR-301a-3p might play an important role in the progression of post-RALP-related or CIH-mediated ED by targeting PTEN and TLR4 thereby affecting the expression levels of α-SMA, eNOS, cell autophagy and apoptosis. Despite miR-301a-3p/PTEN and miR-301a-3p/TLR4 signaling pathway needing further investigation, our findings suggest that miR-301a-3p should be considered as a new therapeutic target for ED treatment.

Abbreviations

erectile dysfunction: ED

obstructive sleep apnea: OSA

adipose-derived mesenchymal stem cells: ADSCs

Sprague Dawley: SD

chronic intermittent hypoxia: CIH

corpus cavernous smooth muscle cells: CCSMCs

alpha Smooth Muscle Actin: α-SMA

phosphatase and tensin homolog: PTEN

Toll-like receptor 4: TLR4

robotic-assisted laparoscopic radical prostatectomy: RALP

cavernous nerve: CN

neuronal nitric oxide synthase: nNOS

endothelial nitric oxide synthase: eNOS

guanylate cyclase: GC

guanosine triphosphate: GTP

cyclic guanosine monophosphate: cGMP

phosphodiesterase type 5: PDE-5

microRNAs: miRNAs

mesenchymal stem cells: MSCs

type 2 diabetes mellitus-associated erectile dysfunction: T2DMED

intracavernous pressure: ICP

arterial pressure: AP

mean carotid artery pressure: MAP

Declarations

Ethics approval and consent to participate

The study has been examined and certified by the Ethics Committee of Shanghai Ninth People's Hospital of Shanghai Jiao Tong University, and informed consent was obtained from all participants included in the study, in agreement with institutional guidelines.

Consent for publication

Written informed consent was obtained from all patients.

Availability of data and materials

The data generated or analyzed during this study are included in this article, or if absent are available from the corresponding author upon reasonable request.

Competing interests

The authors declare that they have no competing interests.

Funding

This work was financially supported by Seed Founding of Shanghai Ninth People's Hospital, Shanghai Jiao Tong university School of Medicine (JYZZ021).

Author Contribution

Xin Gu and Bin Xu designed experiments; Li Liang, Dachao Zheng, Qinghong Xi, Hua Bao and Yufei Gu performed experiments. Chao Lu and Wengfeng Li analysed the results; Li Liang and Dachao Zheng wrote the manuscript. Xin Gu and Yuanshen Mao revised and approved the submitted version.

Acknowledgements

We thank HOME for Researchers (http://www.home-for-researchers.com/static/index.html#/retouch_draw) for editing this manuscript.

References

1. Shamloul R, Ghanem H: **Erectile dysfunction**. *Lancet* 2013, **381**(9861):153-165.
2. Lue TF: **Erectile dysfunction**. *The New England journal of medicine* 2000, **342**(24):1802-1813.
3. Braun M, Wassmer G, Klotz T, Reifenrath B, Mathers M, Engelmann U: **Epidemiology of erectile dysfunction: results of the 'Cologne Male Survey'**. *International journal of impotence research* 2000, **12**(6):305-311.
4. Lewis RW, Fugl-Meyer KS, Corona G, Hayes RD, Laumann EO, Moreira ED, Jr., Rellini AH, Segraves T: **Definitions/epidemiology/risk factors for sexual dysfunction**. *The journal of sexual medicine* 2010, **7**(4 Pt 2):1598-1607.
5. Bokhour BG, Clark JA, Inui TS, Silliman RA, Talcott JA: **Sexuality after treatment for early prostate cancer: exploring the meanings of "erectile dysfunction"**. *Journal of general internal medicine* 2001, **16**(10):649-655.
6. Siegel T, Moul JW, Spevak M, Alvord WG, Costabile RA: **The development of erectile dysfunction in men treated for prostate cancer**. *The Journal of urology* 2001, **165**(2):430-435.
7. Gu X, Thakker PU, Matz EL, Terlecki RP, Marini FC, Allickson JG, Lue TF, Lin G, Atala A, Yoo JJ *et al*: **Dynamic Changes in Erectile Function and Histological Architecture After Intracorporal Injection of Human Placental Stem Cells in a Pelvic Neurovascular Injury Rat Model**. *The journal of sexual medicine* 2020, **17**(3):400-411.

8. Drager LF, Jun JC, Polotsky VY: **Metabolic consequences of intermittent hypoxia: relevance to obstructive sleep apnea**. *Best practice & research Clinical endocrinology & metabolism* 2010, **24**(5):843-851.
9. Chiang AA: **Obstructive sleep apnea and chronic intermittent hypoxia: a review**. *The Chinese journal of physiology* 2006, **49**(5):234-243.
10. Fanfulla F, Malaguti S, Montagna T, Salvini S, Bruschi C, Crotti P, Casale R, Rampulla C: **Erectile dysfunction in men with obstructive sleep apnea: an early sign of nerve involvement**. *Sleep* 2000, **23**(6):775-781.
11. Soukhova-O'Hare GK, Shah ZA, Lei Z, Nozdrachev AD, Rao CV, Gozal D: **Erectile dysfunction in a murine model of sleep apnea**. *American journal of respiratory and critical care medicine* 2008, **178**(6):644-650.
12. Yu DP, Liu XH, Wei AY: **Effect of chronic hypoxia on penile erectile function in rats**. *Genetics and molecular research : GMR* 2015, **14**(3):10482-10489.
13. Burnett AL: **The role of nitric oxide in erectile dysfunction: implications for medical therapy**. *Journal of clinical hypertension* 2006, **8**(12 Suppl 4):53-62.
14. Carter JE: **Anterior ischemic optic neuropathy and stroke with use of PDE-5 inhibitors for erectile dysfunction: cause or coincidence?** *Journal of the neurological sciences* 2007, **262**(1-2):89-97.
15. Jeong HH, Piao S, Ha JN, Kim IG, Oh SH, Lee JH, Cho HJ, Hong SH, Kim SW, Lee JY: **Combined therapeutic effect of udenafil and adipose-derived stem cell (ADSC)/brain-derived neurotrophic factor (BDNF)-membrane system in a rat model of cavernous nerve injury**. *Urology* 2013, **81**(5):1108 e1107-1114.
16. Wu H, Tang WH, Zhao LM, Liu DF, Yang YZ, Zhang HT, Zhang Z, Hong K, Lin HC, Jiang H: **Nanotechnology-assisted adipose-derived stem cell (ADSC) therapy for erectile dysfunction of cavernous nerve injury: In vivo cell tracking, optimized injection dosage, and functional evaluation**. *Asian journal of andrology* 2018, **20**(5):442-447.
17. Ferguson SW, Nguyen J: **Exosomes as therapeutics: The implications of molecular composition and exosomal heterogeneity**. *Journal of controlled release : official journal of the Controlled Release Society* 2016, **228**:179-190.
18. Jiang M, Wang H, Jin M, Yang X, Ji H, Jiang Y, Zhang H, Wu F, Wu G, Lai X *et al*: **Exosomes from MiR-30d-5p-ADSCs Reverse Acute Ischemic Stroke-Induced, Autophagy-Mediated Brain Injury by Promoting M2 Microglial/Macrophage Polarization**. *Cellular physiology and biochemistry : international journal of experimental cellular physiology, biochemistry, and pharmacology* 2018, **47**(2):864-878.
19. Katakowski M, Buller B, Zheng X, Lu Y, Rogers T, Osobamiro O, Shu W, Jiang F, Chopp M: **Exosomes from marrow stromal cells expressing miR-146b inhibit glioma growth**. *Cancer letters* 2013, **335**(1):201-204.
20. Luo Q, Guo D, Liu G, Chen G, Hang M, Jin M: **Exosomes from MiR-126-Overexpressing Adscs Are Therapeutic in Relieving Acute Myocardial Ischaemic Injury**. *Cellular physiology and biochemistry :*

international journal of experimental cellular physiology, biochemistry, and pharmacology 2017, **44**(6):2105-2116.

21. Xin H, Li Y, Buller B, Katakowski M, Zhang Y, Wang X, Shang X, Zhang ZG, Chopp M: **Exosome-mediated transfer of miR-133b from multipotent mesenchymal stromal cells to neural cells contributes to neurite outgrowth**. *Stem cells* 2012, **30**(7):1556-1564.
22. Chen F, Zhang H, Wang Z, Ding W, Zeng Q, Liu W, Huang C, He S, Wei A: **Adipose-Derived Stem Cell-Derived Exosomes Ameliorate Erectile Dysfunction in a Rat Model of Type 2 Diabetes**. *The journal of sexual medicine* 2017, **14**(9):1084-1094.
23. Li M, Lei H, Xu Y, Li H, Yang B, Yu C, Yuan Y, Fang D, Xin Z, Guan R: **Exosomes derived from mesenchymal stem cells exert therapeutic effect in a rat model of cavernous nerves injury**. *Andrology* 2018, **6**(6):927-935.
24. Ouyang X, Han X, Chen Z, Fang J, Huang X, Wei H: **MSC-derived exosomes ameliorate erectile dysfunction by alleviation of corpus cavernosum smooth muscle apoptosis in a rat model of cavernous nerve injury**. *Stem cell research & therapy* 2018, **9**(1):246.
25. Zhu LL, Huang X, Yu W, Chen H, Chen Y, Dai YT: **Transplantation of adipose tissue-derived stem cell-derived exosomes ameliorates erectile function in diabetic rats**. *Andrologia* 2018, **50**(2).
26. Alacam H, Akgun S, Akca H, Ozturk O, Kabukcu BB, Herken H: **miR-181b-5p, miR-195-5p and miR-301a-3p are related with treatment resistance in schizophrenia**. *Psychiatry research* 2016, **245**:200-206.
27. Lettlova S, Brynychova V, Blecha J, Vrana D, Vondrusova M, Soucek P, Truksa J: **MiR-301a-3p Suppresses Estrogen Signaling by Directly Inhibiting ESR1 in ERalpha Positive Breast Cancer**. *Cellular physiology and biochemistry : international journal of experimental cellular physiology, biochemistry, and pharmacology* 2018, **46**(6):2601-2615.
28. Lu Y, Gao W, Zhang C, Wen S, Huangfu H, Kang J, Wang B: **Hsa-miR-301a-3p Acts as an Oncogene in Laryngeal Squamous Cell Carcinoma via Target Regulation of Smad4**. *Journal of Cancer* 2015, **6**(12):1260-1275.
29. Xia X, Zhang K, Cen G, Jiang T, Cao J, Huang K, Huang C, Zhao Q, Qiu Z: **MicroRNA-301a-3p promotes pancreatic cancer progression via negative regulation of SMAD4**. *Oncotarget* 2015, **6**(25):21046-21063.
30. Pan F, You J, Liu Y, Qiu X, Yu W, Ma J, Pan L, Zhang A, Zhang Q: **Differentially expressed microRNAs in the corpus cavernosum from a murine model with type 2 diabetes mellitus-associated erectile dysfunction**. *Molecular genetics and genomics : MGG* 2016, **291**(6):2215-2224.
31. Gu X, Shi H, Matz E, Zhong L, Long T, Clouse C, Li W, Chen D, Chung H, Murphy S *et al*: **Long-term therapeutic effect of cell therapy on improvement in erectile function in a rat model with pelvic neurovascular injury**. *BJU international* 2019, **124**(1):145-154.
32. Hirshkowitz M, Karacan I, Arcasoy MO, Acik G, Narter EM, Williams RL: **Prevalence of sleep apnea in men with erectile dysfunction**. *Urology* 1990, **36**(3):232-234.

33. Wespes E: **Smooth muscle pathology and erectile dysfunction**. *International journal of impotence research* 2002, **14 Suppl 1**:S17-21.

34. Zhu GQ, Jeon SH, Bae WJ, Choi SW, Jeong HC, Kim KS, Kim SJ, Cho HJ, Ha US, Hong SH *et al*: **Efficient Promotion of Autophagy and Angiogenesis Using Mesenchymal Stem Cell Therapy Enhanced by the Low-Energy Shock Waves in the Treatment of Erectile Dysfunction**. *Stem cells international* 2018, **2018**:1302672.

Figures

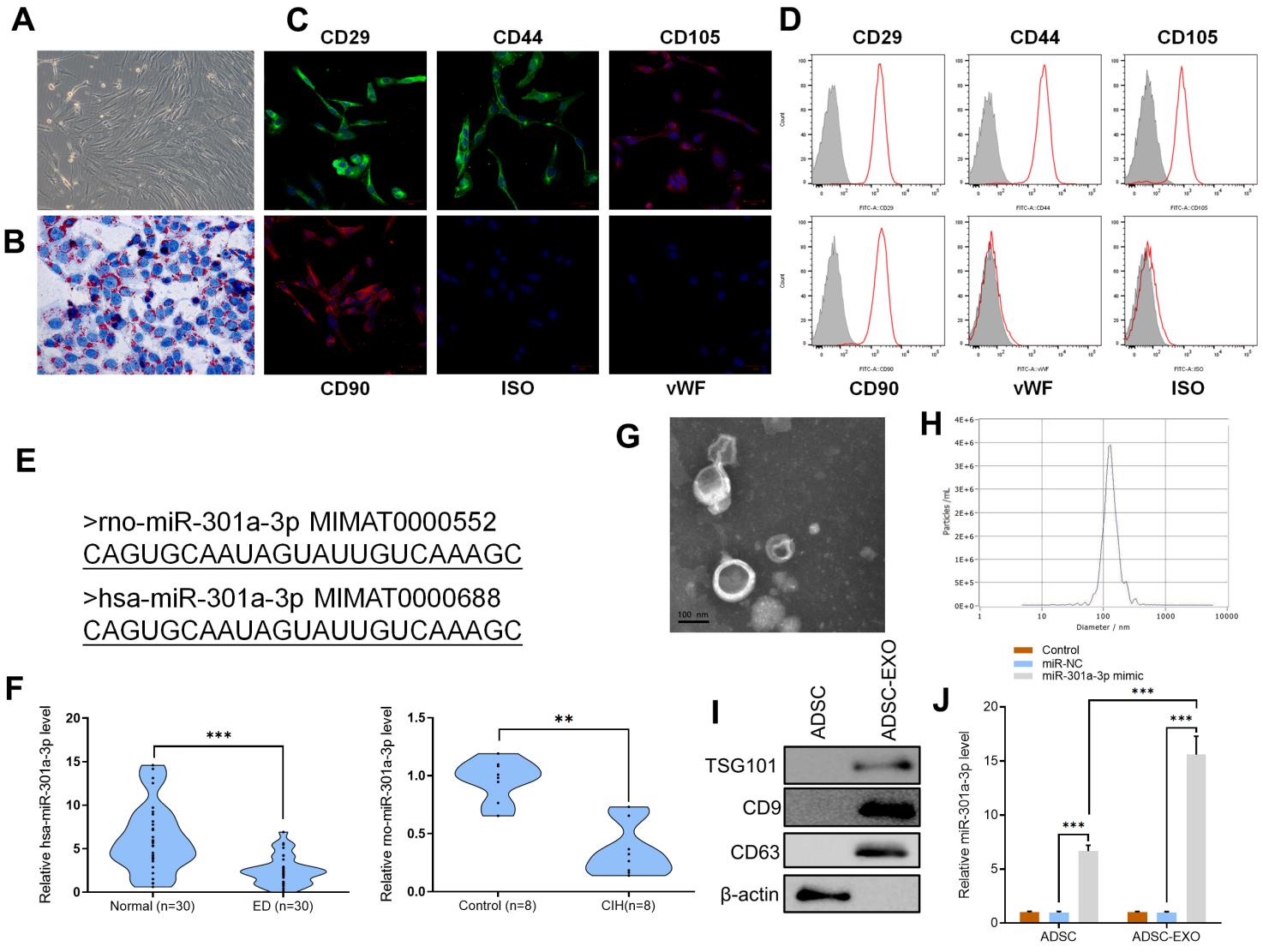

Figure 1

A) ADSCs were collected from adipose tissues of SD rats. ADSCs displayed a typical cobblestone-like morphology under microscope. B) Adipose cells were confirmed with Oil Red O staining. C) ADSCs were positive for the mesenchymal stem cell (MSC) markers CD29, CD34, CD44, CD90 and CD 105. D) Flow cytometry analysis of the surface markers in ADSCs. E) Sequence of rno-miR-301a-3p and has-miR-301a-

3p. F) The expression levels of rno-miR-301a-3p and has-miR-301a-3p in serum samples from patients and SD rats, respectively (**p <0.01, ***p <0.001). G and H) Images of ADSC-derived exosomes and nanoparticle tracking analysis of exosomes. I) Protein levels of TSG101, CD9 and CD63 in ADSC and ADSC-derived exosomes as determined by Western blotting. J) RT-qPCR results of miR-301a level in ADSC and ADSC-derived exosomes. Data are expressed as mean ± SD (n = 3 for ADSC analysis; ***p <0.001).

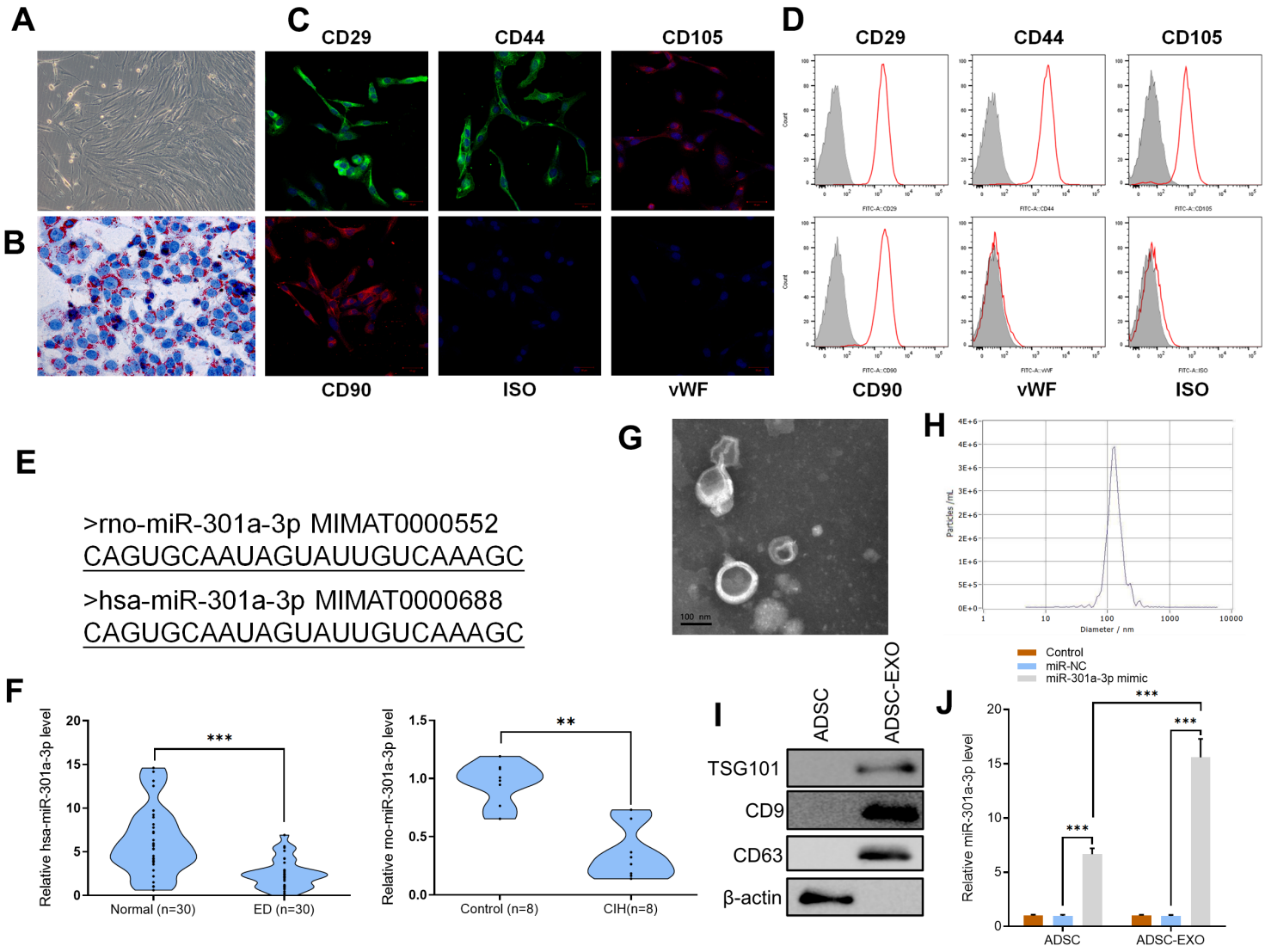

Figure 1

A) ADSCs were collected from adipose tissues of SD rats. ADSCs displayed a typical cobblestone-like morphology under microscope. B) Adipose cells were confirmed with Oil Red O staining. C) ADSCs were positive for the mesenchymal stem cell (MSC) markers CD29, CD34, CD44, CD90 and CD 105. D) Flow cytometry analysis of the surface markers in ADSCs. E) Sequence of rno-miR-301a-3p and has-miR-301a-3p. F) The expression levels of rno-miR-301a-3p and has-miR-301a-3p in serum samples from patients and SD rats, respectively (**p <0.01, ***p <0.001). G and H) Images of ADSC-derived exosomes and nanoparticle tracking analysis of exosomes. I) Protein levels of TSG101, CD9 and CD63 in ADSC and ADSC-derived exosomes as determined by Western blotting. J) RT-qPCR results of miR-301a level in

ADSC and ADSC-derived exosomes. Data are expressed as mean ± SD (n = 3 for ADSC analysis; ***p <0.001).

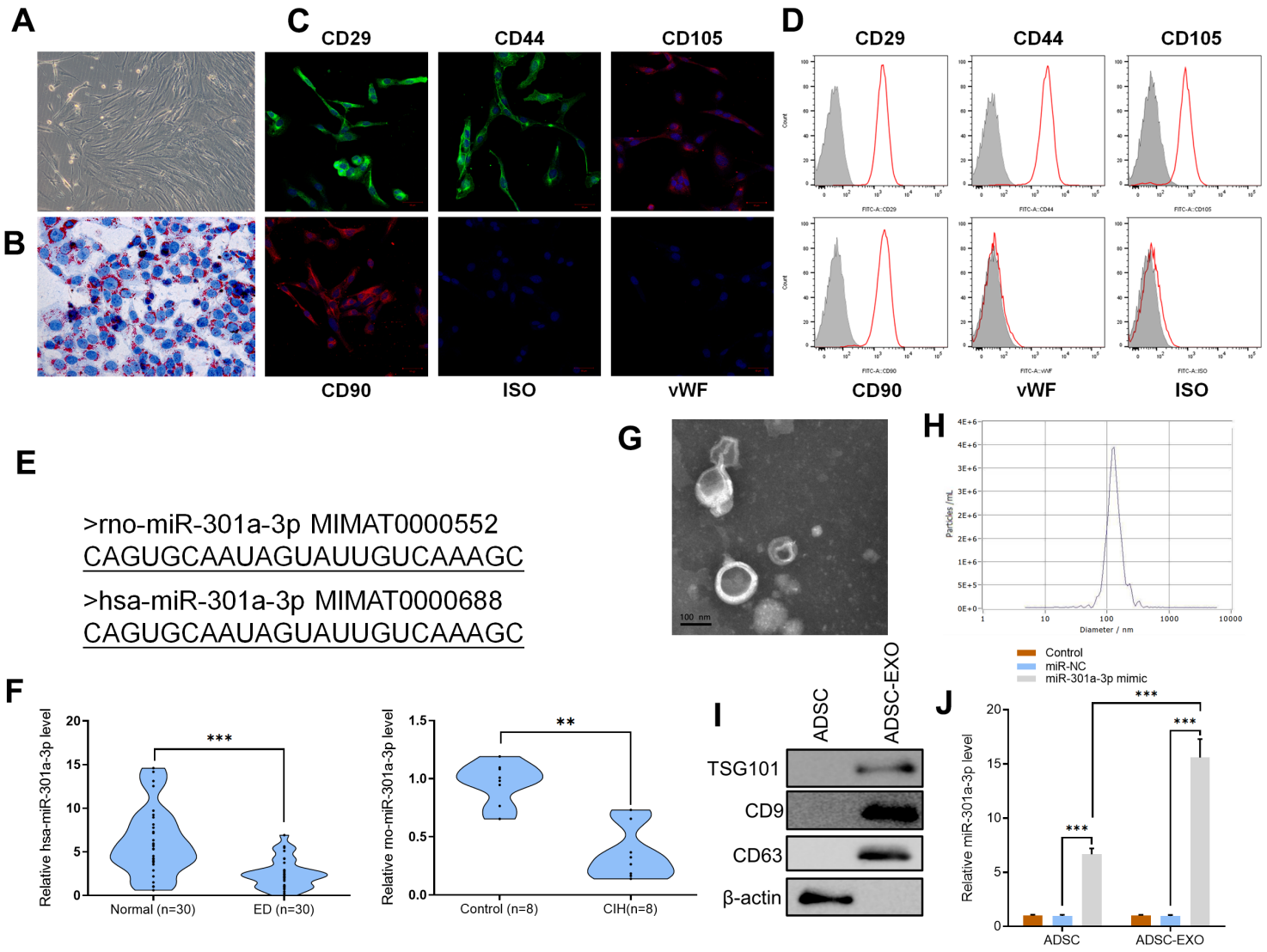

Figure 1

A) ADSCs were collected from adipose tissues of SD rats. ADSCs displayed a typical cobblestone-like morphology under microscope. B) Adipose cells were confirmed with Oil Red O staining. C) ADSCs were positive for the mesenchymal stem cell (MSC) markers CD29, CD34, CD44, CD90 and CD 105. D) Flow cytometry analysis of the surface markers in ADSCs. E) Sequence of rno-miR-301a-3p and has-miR-301a-3p. F) The expression levels of rno-miR-301a-3p and has-miR-301a-3p in serum samples from patients and SD rats, respectively (**p <0.01, ***p <0.001). G and H) Images of ADSC-derived exosomes and nanoparticle tracking analysis of exosomes. I) Protein levels of TSG101, CD9 and CD63 in ADSC and ADSC-derived exosomes as determined by Western blotting. J) RT-qPCR results of miR-301a level in ADSC and ADSC-derived exosomes. Data are expressed as mean ± SD (n = 3 for ADSC analysis; ***p <0.001).

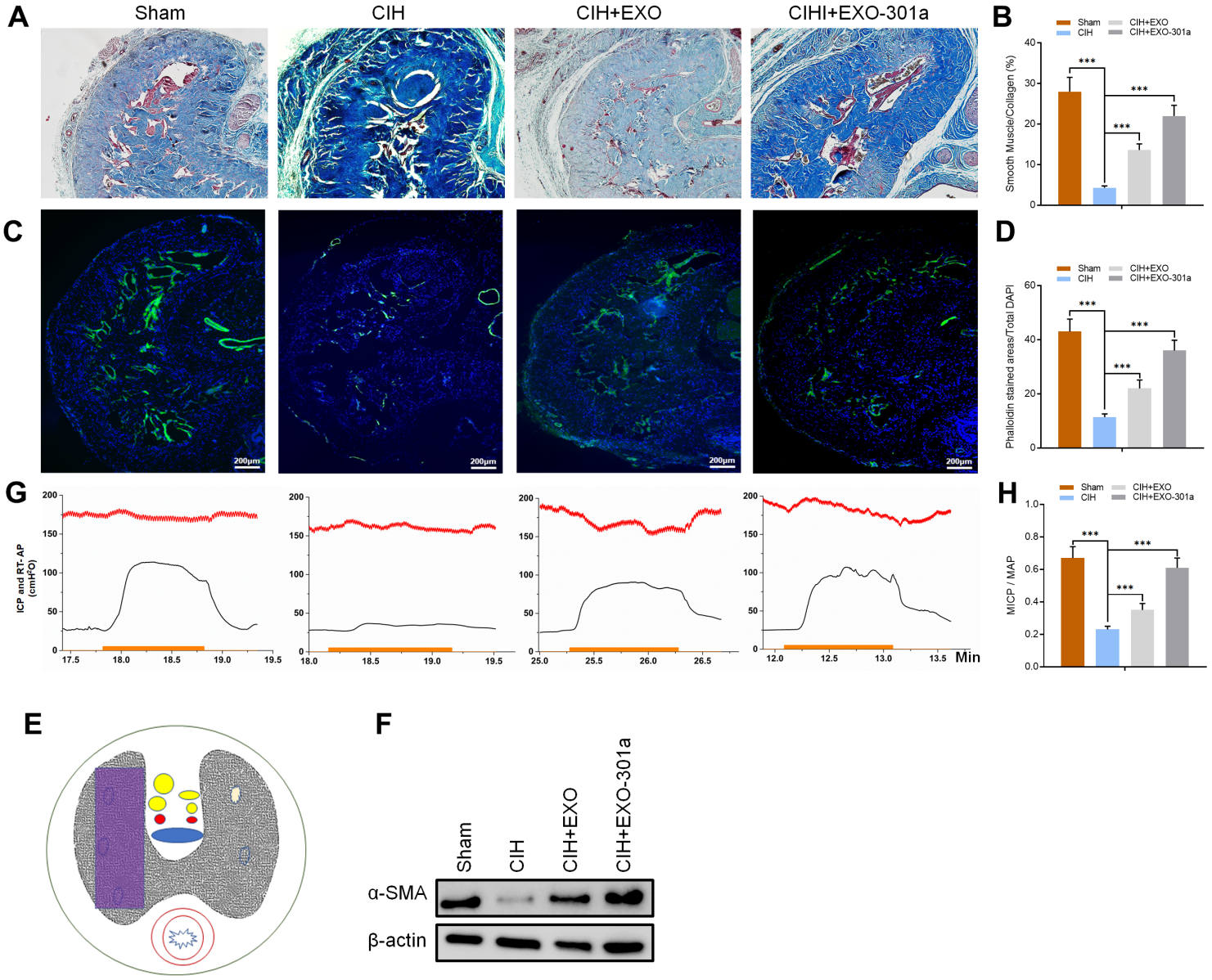

Figure 2

Rats were dived into 4 groups: Sham, CIH exposure, CIH + exosomes from untreated ADSCs (Exo) and CIH + miR-301a-3p-enriched exosomes (Exo-301a). A and B) Results of Masson trichrome staining for actin (red) and collagen (blue). C and D) Results of Phalloidin (green) and DAPI (blue)staining in SD rats. E) The purple rectangle denotes the area of the penis selected for an area for histology analysis. F) Protein levels of α-SMA in Sham, CIH, CIH+EXO, CIH+EXO-301a groups as determined by Western blotting. G and H) Results of ICP and RT-AP measurement in all four groups. The ICP is indicated with green curve. The red curve denotes the real-time AP during electrostimulation. The orange bar denotes the 60s cavernous nerve electrical stimulation. Data are expressed as mean ± SD (n = 6; ***p <0.001).

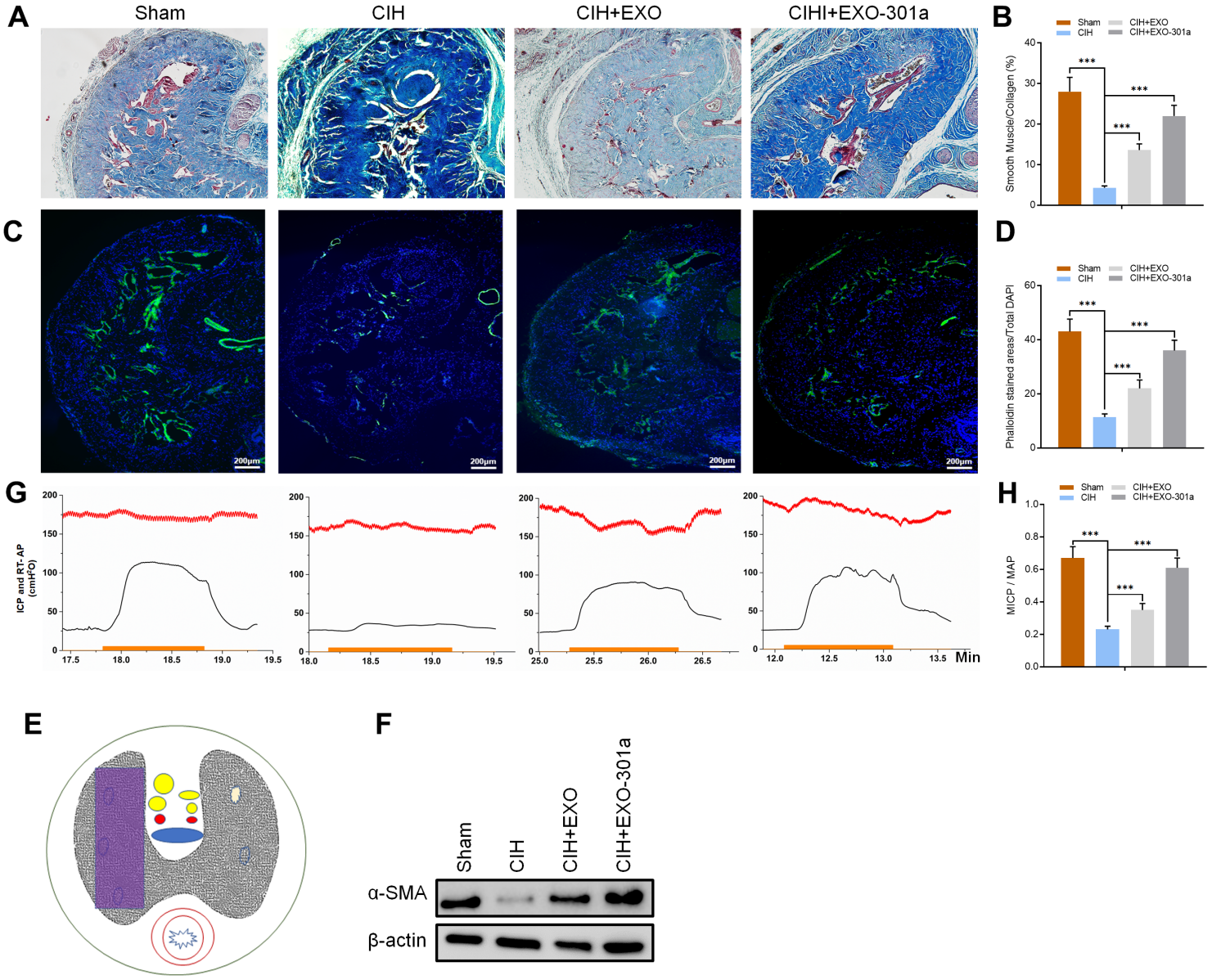

Figure 2

Rats were dived into 4 groups: Sham, CIH exposure, CIH + exosomes from untreated ADSCs (Exo) and CIH + miR-301a-3p-enriched exosomes (Exo-301a). A and B) Results of Masson trichrome staining for actin (red) and collagen (blue). C and D) Results of Phalloidin (green) and DAPI (blue)staining in SD rats. E) The purple rectangle denotes the area of the penis selected for an area for histology analysis. F) Protein levels of α-SMA in Sham, CIH, CIH+EXO, CIH+EXO-301a groups as determined by Western blotting. G and H) Results of ICP and RT-AP measurement in all four groups. The ICP is indicated with green curve. The red curve denotes the real-time AP during electrostimulation. The orange bar denotes the 60s cavernous nerve electrical stimulation. Data are expressed as mean ± SD (n = 6; ***p <0.001).

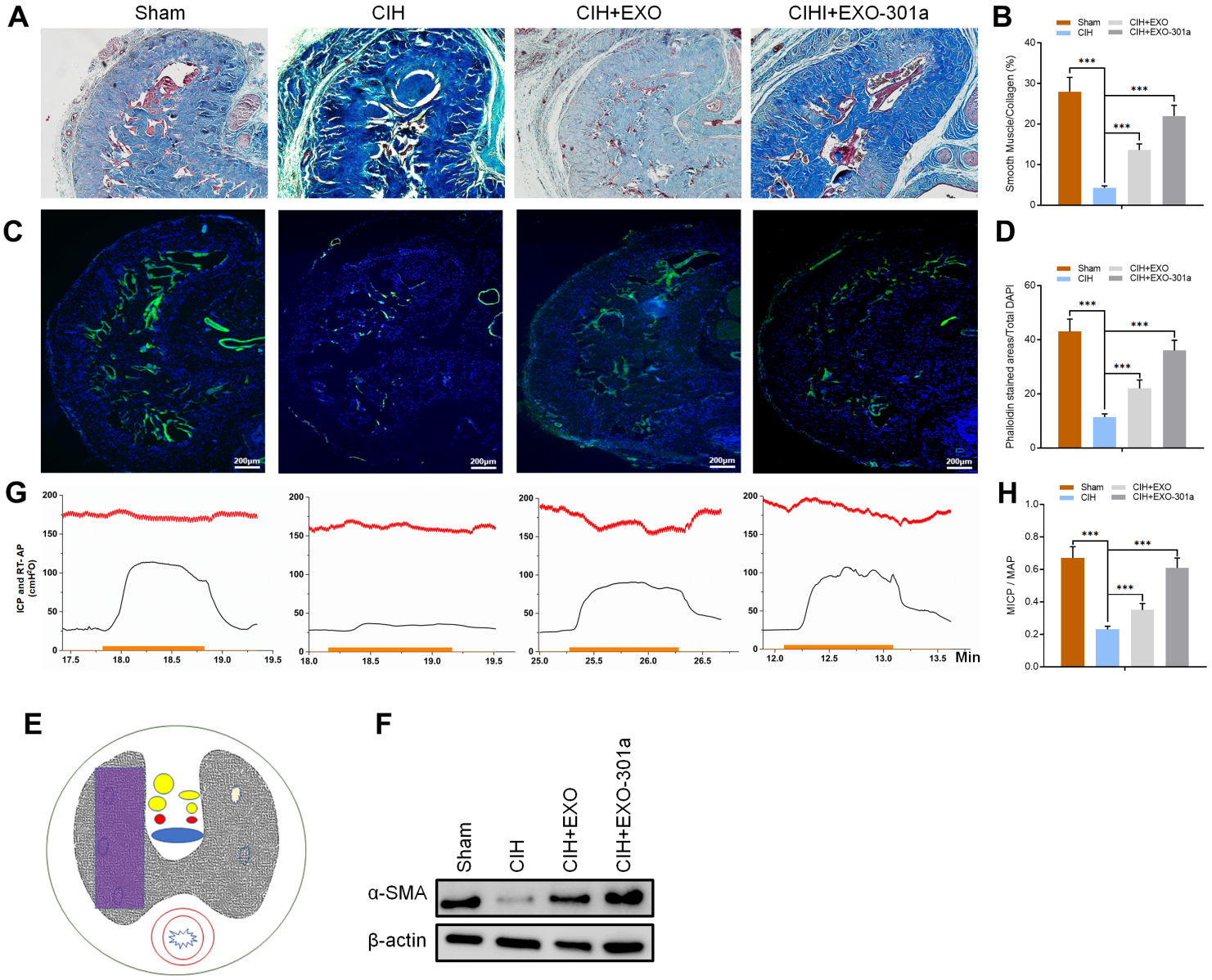

Figure 2

Rats were dived into 4 groups: Sham, CIH exposure, CIH + exosomes from untreated ADSCs (Exo) and CIH + miR-301a-3p-enriched exosomes (Exo-301a). A and B) Results of Masson trichrome staining for actin (red) and collagen (blue). C and D) Results of Phalloidin (green) and DAPI (blue)staining in SD rats. E) The purple rectangle denotes the area of the penis selected for an area for histology analysis. F) Protein levels of α-SMA in Sham, CIH, CIH+EXO, CIH+EXO-301a groups as determined by Western blotting. G and H) Results of ICP and RT-AP measurement in all four groups. The ICP is indicated with green curve. The red curve denotes the real-time AP during electrostimulation. The orange bar denotes the 60s cavernous nerve electrical stimulation. Data are expressed as mean ± SD (n = 6; ***p <0.001).

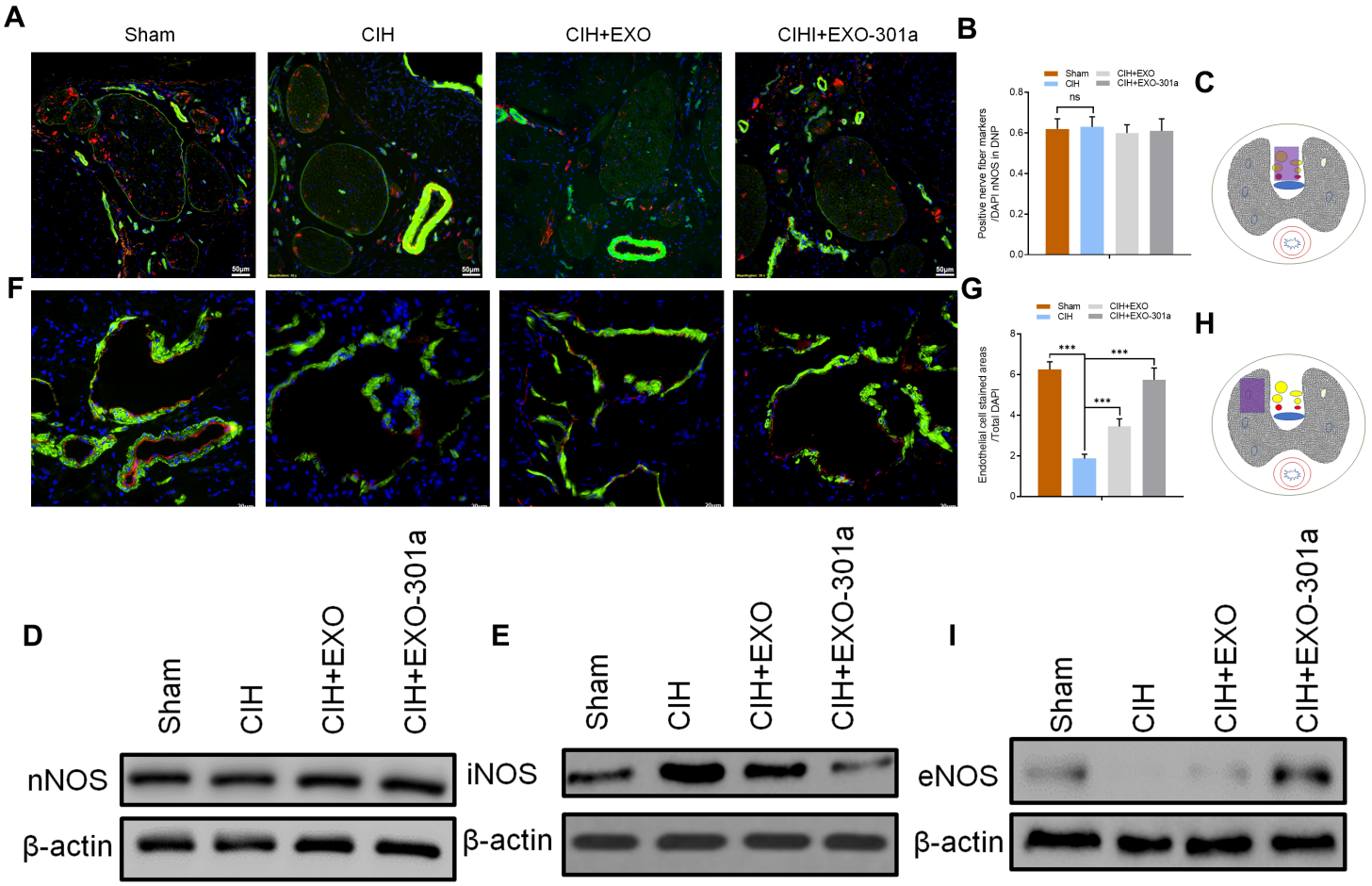

Figure 3

Rats were dived into 4 groups: Sham, CIH exposure, CIH + exosomes from untreated ADSCs (Exo) and CIH + miR-301a-3p-enriched exosomes (Exo-301a).A, B and C) The DNP area selected for nNOS (red) analysis and results of Phalloidin (green) and DAPI (blue) staining. The purple rectangle denotes the area of the penis selected for an area for histology analysis. D and E) Protein levels of nNOS and iNOS in DNP as determined by Western blotting. F, G and H) The area selected for eNOS(red) analysis and results of Phalloidin (green) and DAPI (blue). The purple rectangle denotes the area of the penis selected for analysis. I) Protein levels of eNOS as determined by Western blotting. Data are expressed as mean ± SD (n = 6; **p <0.01, ***p <0.001, ns mean none significant).

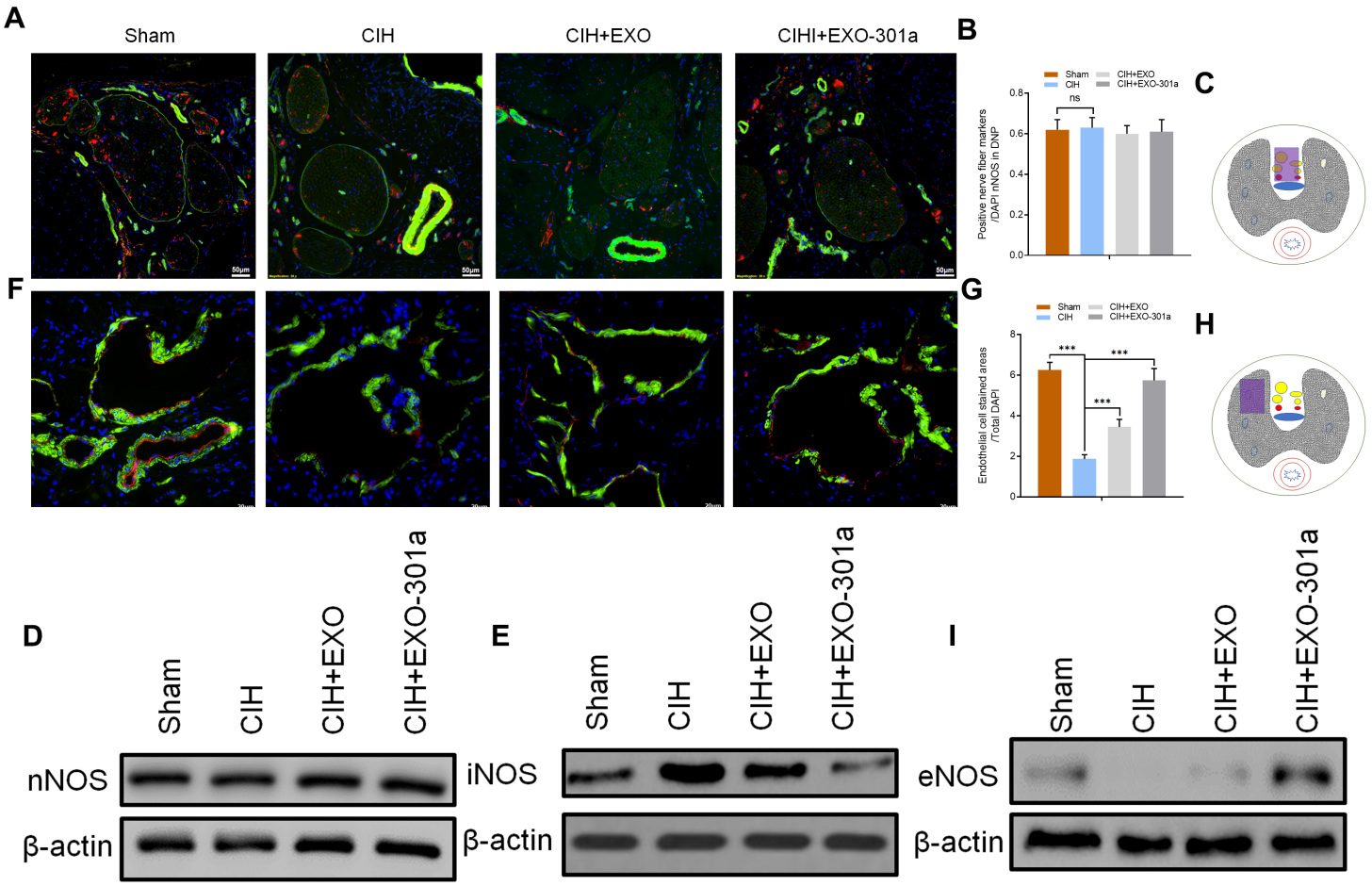

Figure 3

Rats were dived into 4 groups: Sham, CIH exposure, CIH + exosomes from untreated ADSCs (Exo) and CIH + miR-301a-3p-enriched exosomes (Exo-301a).A, B and C) The DNP area selected for nNOS (red) analysis and results of Phalloidin (green) and DAPI (blue) staining. The purple rectangle denotes the area of the penis selected for an area for histology analysis. D and E) Protein levels of nNOS and iNOS in DNP as determined by Western blotting. F, G and H) The area selected for eNOS(red) analysis and results of Phalloidin (green) and DAPI (blue). The purple rectangle denotes the area of the penis selected for analysis. I) Protein levels of eNOS as determined by Western blotting. Data are expressed as mean ± SD (n = 6; **p <0.01, ***p <0.001, ns mean none significant).

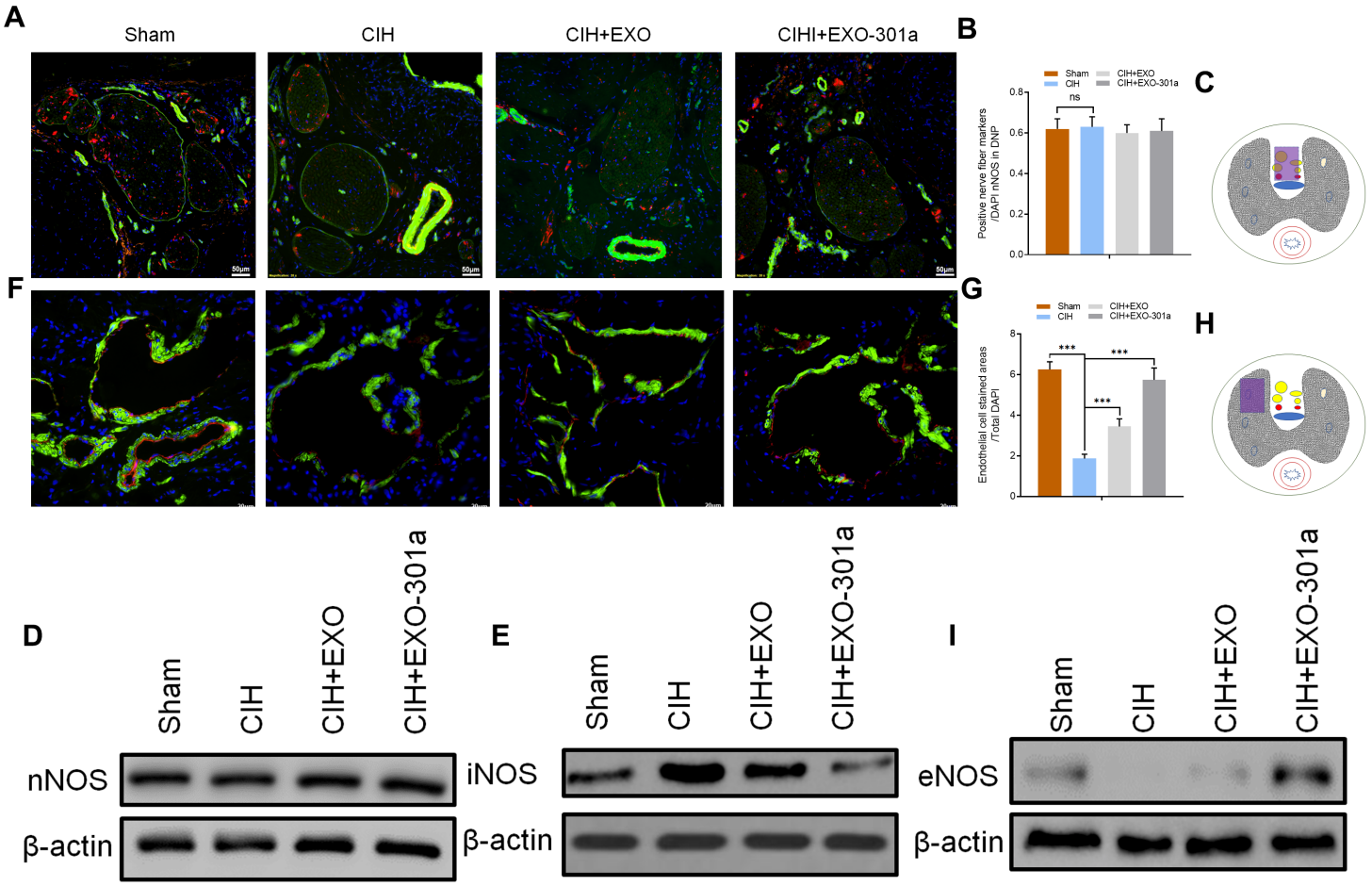

Figure 3

Rats were dived into 4 groups: Sham, CIH exposure, CIH + exosomes from untreated ADSCs (Exo) and CIH + miR-301a-3p-enriched exosomes (Exo-301a).A, B and C) The DNP area selected for nNOS (red) analysis and results of Phalloidin (green) and DAPI (blue) staining. The purple rectangle denotes the area of the penis selected for an area for histology analysis. D and E) Protein levels of nNOS and iNOS in DNP as determined by Western blotting. F, G and H) The area selected for eNOS(red) analysis and results of Phalloidin (green) and DAPI (blue). The purple rectangle denotes the area of the penis selected for analysis. I) Protein levels of eNOS as determined by Western blotting. Data are expressed as mean ± SD (n = 6; **p <0.01, ***p <0.001, ns mean none significant).

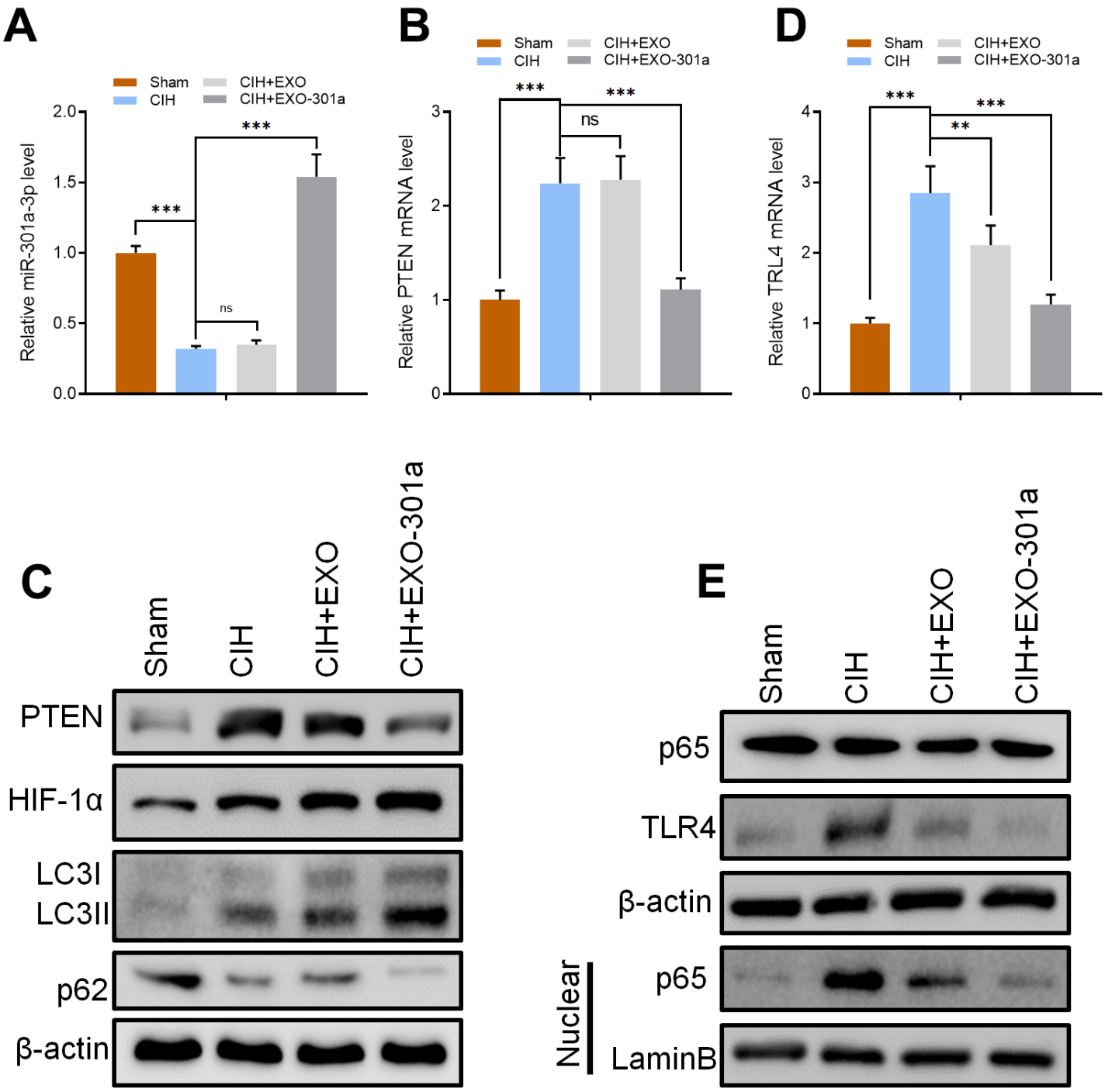

Figure 4

Rats were dived into 4 groups: Sham, CIH exposure, CIH + exosomes from untreated ADSCs (Exo) and CIH + miR-301a-3p-enriched exosomes (Exo-301a).A, B and D) RT-qPCR results of miR-301a-3p, PTEN and TLR4 in Sham, CIH, CIH+EXO, CIH+EXO-301a in DNP. C and E) Protein levels of PTEN, TLR4, HIF-1α, LC3I/II, p62 and p65 in DNP as measured by Western blotting. Data are expressed as mean ± SD (n = 6; **p <0.01, ***p <0.001, ns mean none significant).

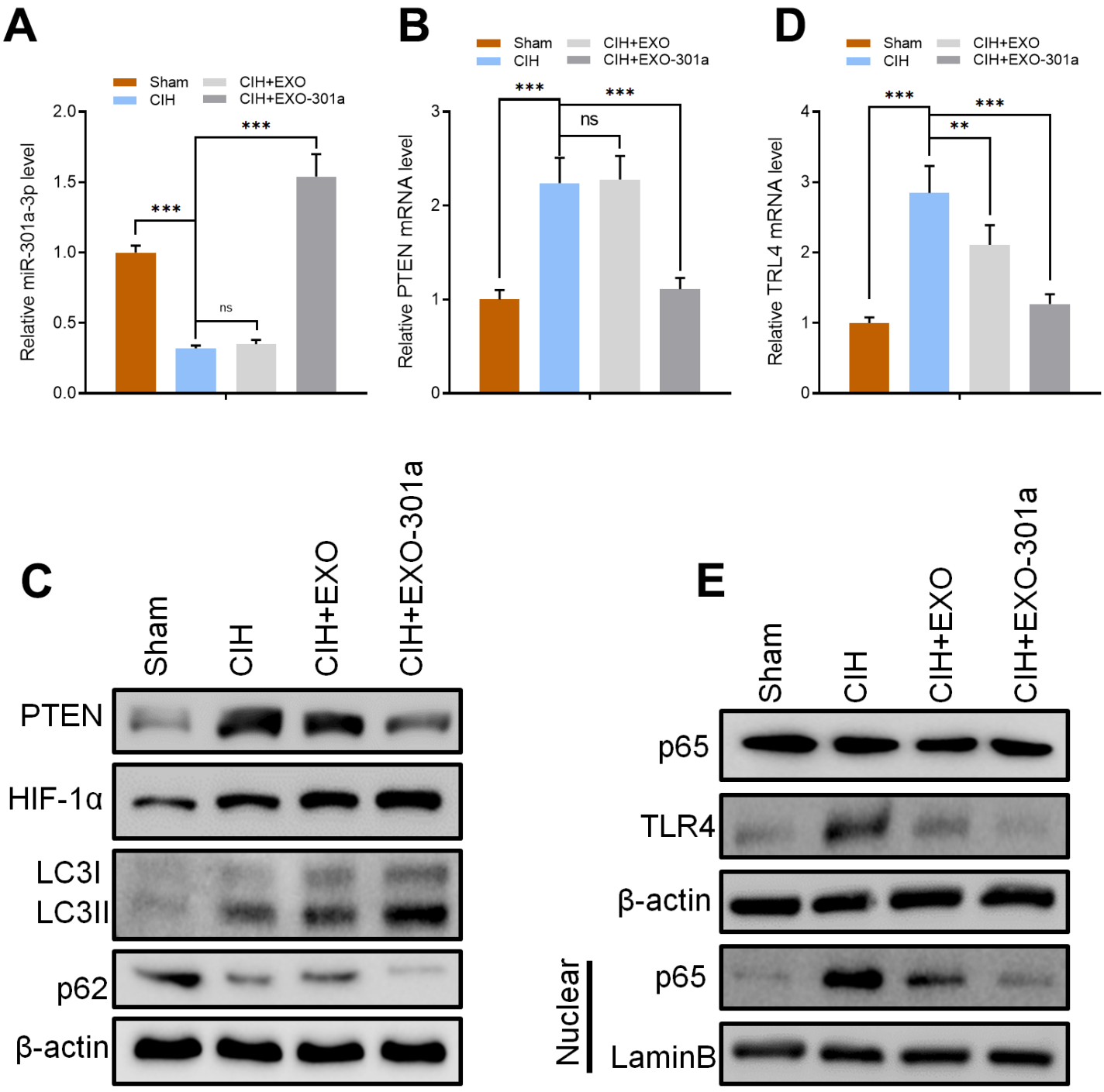

Figure 4

Rats were dived into 4 groups: Sham, CIH exposure, CIH + exosomes from untreated ADSCs (Exo) and CIH + miR-301a-3p-enriched exosomes (Exo-301a).A, B and D) RT-qPCR results of miR-301a-3p, PTEN and TLR4 in Sham, CIH, CIH+EXO, CIH+EXO-301a in DNP. C and E) Protein levels of PTEN, TLR4, HIF-1α, LC3I/II, p62 and p65 in DNP as measured by Western blotting. Data are expressed as mean ± SD (n = 6; **p <0.01, ***p <0.001, ns mean none significant).

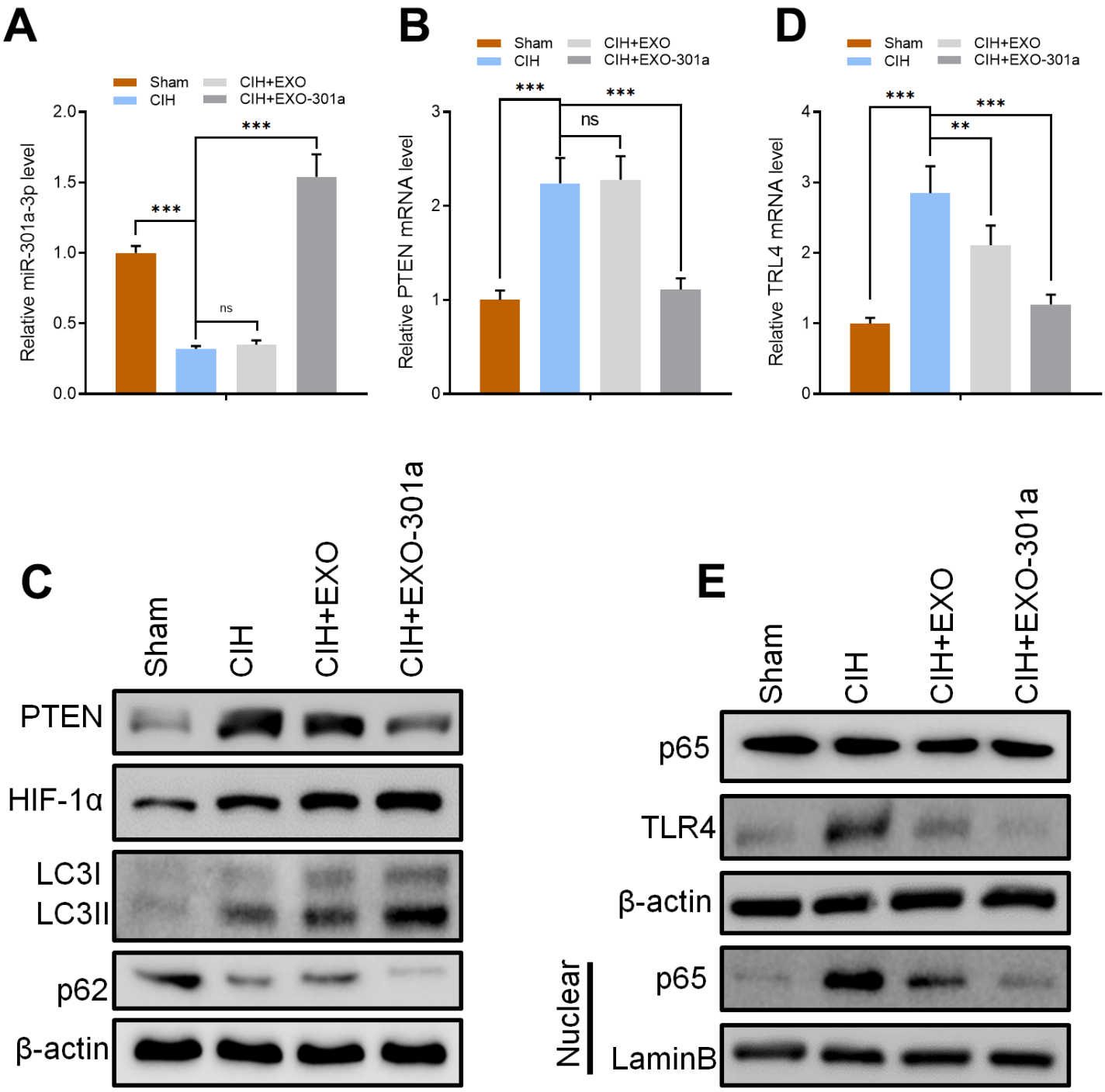

Figure 4

Rats were dived into 4 groups: Sham, CIH exposure, CIH + exosomes from untreated ADSCs (Exo) and CIH + miR-301a-3p-enriched exosomes (Exo-301a).A, B and D) RT-qPCR results of miR-301a-3p, PTEN and TLR4 in Sham, CIH, CIH+EXO, CIH+EXO-301a in DNP. C and E) Protein levels of PTEN, TLR4, HIF-1α, LC3I/II, p62 and p65 in DNP as measured by Western blotting. Data are expressed as mean ± SD (n = 6; **p <0.01, ***p <0.001, ns mean none significant).

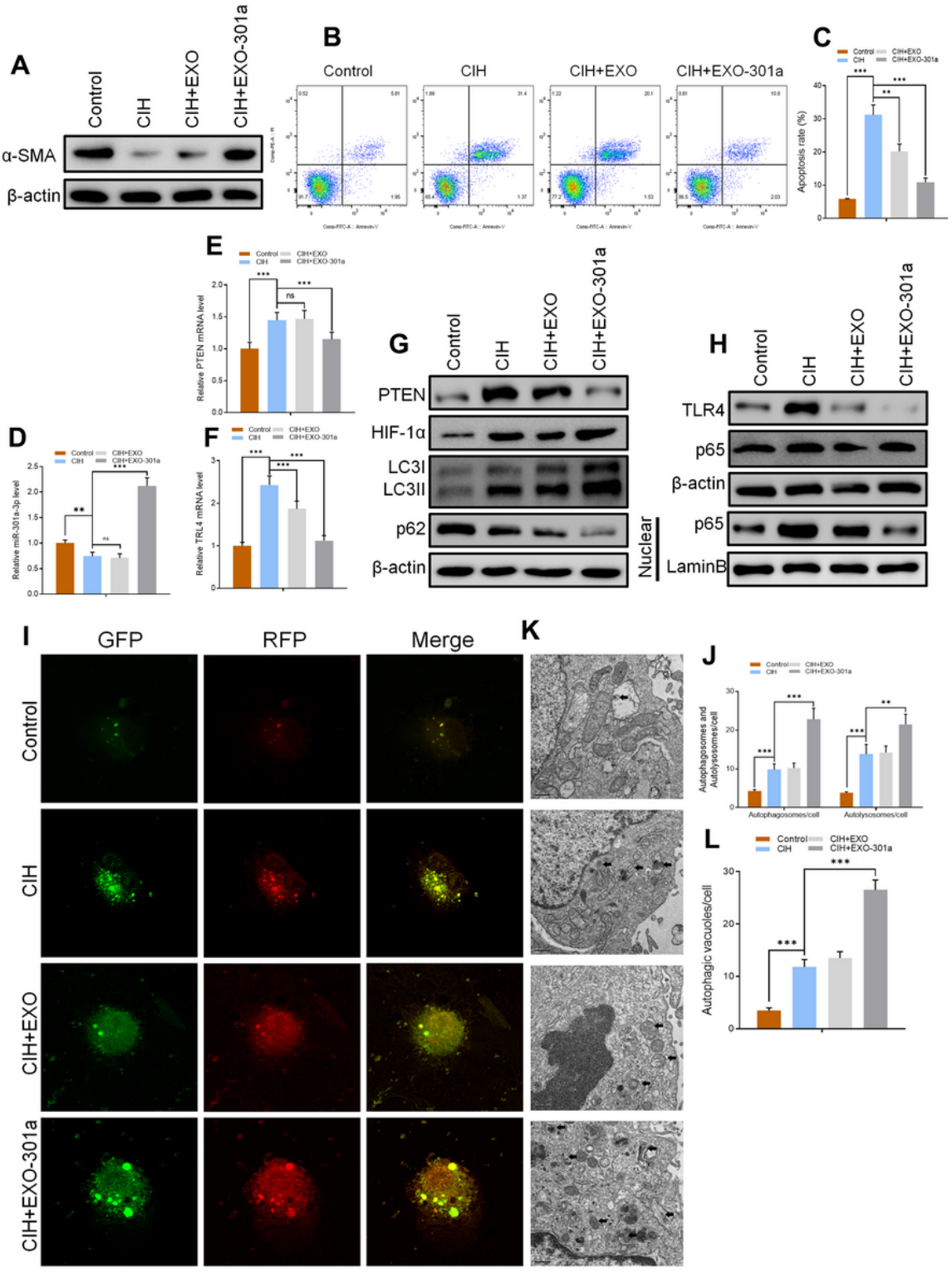

Figure 5

A and C) Results of rno-miR-301a-3p, TLR4 (wt and mut), and PTEN (wt and mut) sequencing. B and D) Luciferase assay of TLR4 (wt and mut), and PTEN (wt and mut) transfected with miR-301a-3p mimic. E) Expression levels of TLR4 and PTEN in control, miR-NC, miR-301a-3p groups as measured by RT-qPCR. F) Protein levels of TLR4 and PTEN in the three groups as measured by Western blotting. Data are expressed as mean ± SD (n = 6; ***p <0.001).

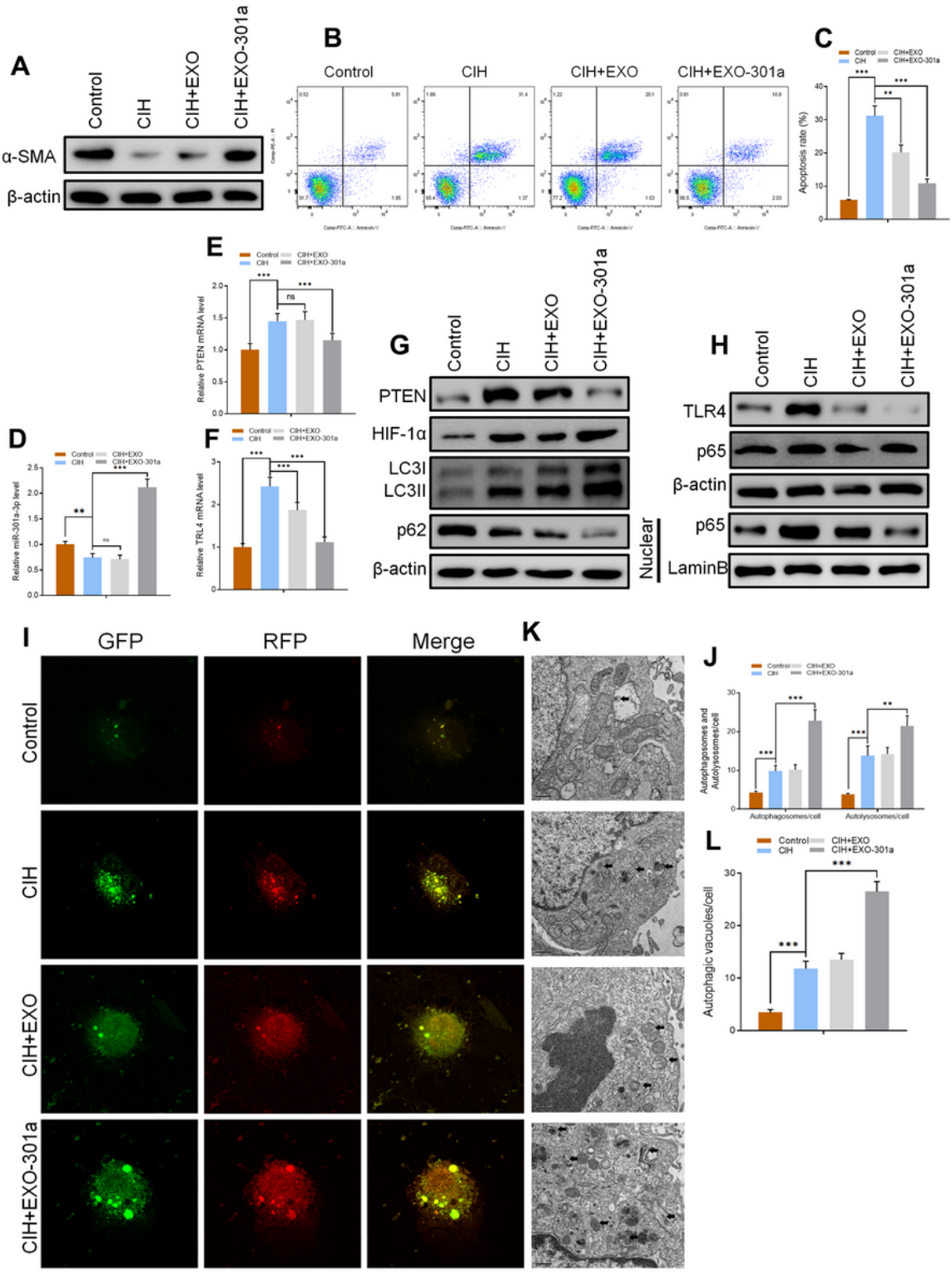

Figure 5

A and C) Results of rno-miR-301a-3p, TLR4 (wt and mut), and PTEN (wt and mut) sequencing. B and D) Luciferase assay of TLR4 (wt and mut), and PTEN (wt and mut) transfected with miR-301a-3p mimic. E) Expression levels of TLR4 and PTEN in control, miR-NC, miR-301a-3p groups as measured by RT-qPCR. F) Protein levels of TLR4 and PTEN in the three groups as measured by Western blotting. Data are expressed as mean ± SD (n = 6; ***p <0.001).

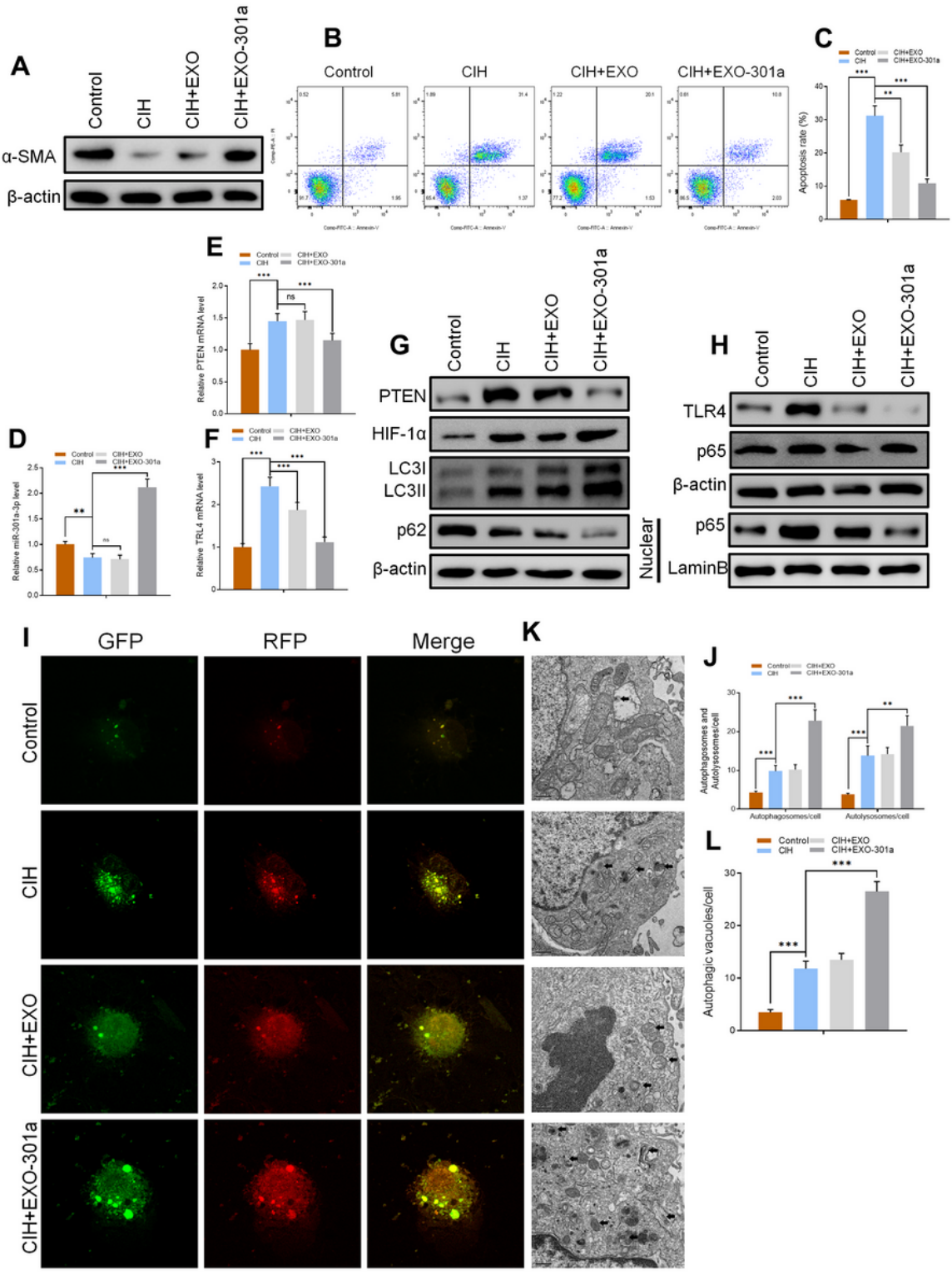

Figure 5

A and C) Results of rno-miR-301a-3p, TLR4 (wt and mut), and PTEN (wt and mut) sequencing. B and D) Luciferase assay of TLR4 (wt and mut), and PTEN (wt and mut) transfected with miR-301a-3p mimic. E) Expression levels of TLR4 and PTEN in control, miR-NC, miR-301a-3p groups as measured by RT-qPCR. F) Protein levels of TLR4 and PTEN in the three groups as measured by Western blotting. Data are expressed as mean ± SD (n = 6; ***p <0.001).

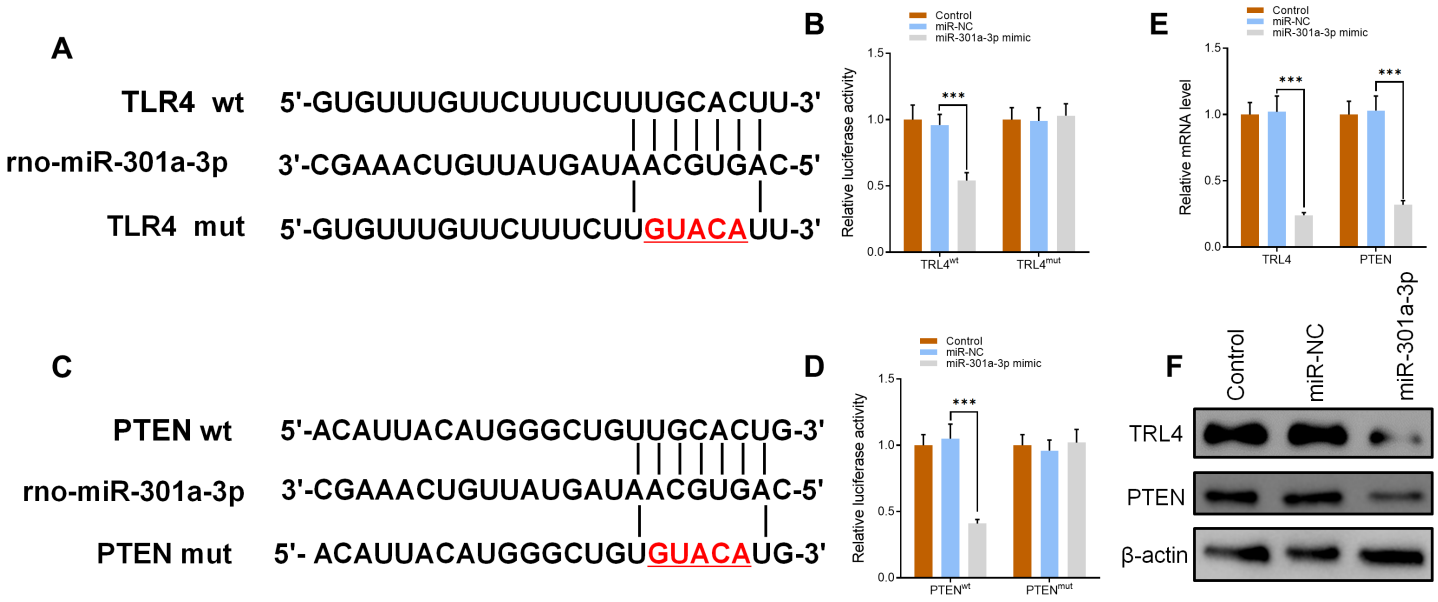

Figure 6

A) Protein levels of α-SMA in control, CIH, CIH+EXO, CIH+EXO-301a groups as measured by Western blotting. B and C) Flow cytometry results of apoptosis rate in all groups. D, E and F) Relative expression of miR-301a-3p, PTEN, and TLR4 level as determined by RT-qPCR. G and H) Protein levels of PTEN, TLR4, HIF-1α, LC3I/II, p62 and p65 in CCSMCs as quantified by Western blotting. I, K, J and L) Results of mRFP-GFP-LC3 staining and quantitation of autophagosomes, autolysosomes, and autophagic vacuoles. Data are expressed as mean ± SD (n = 6; **p <0.01, ***p <0.001, ns mean none significant).

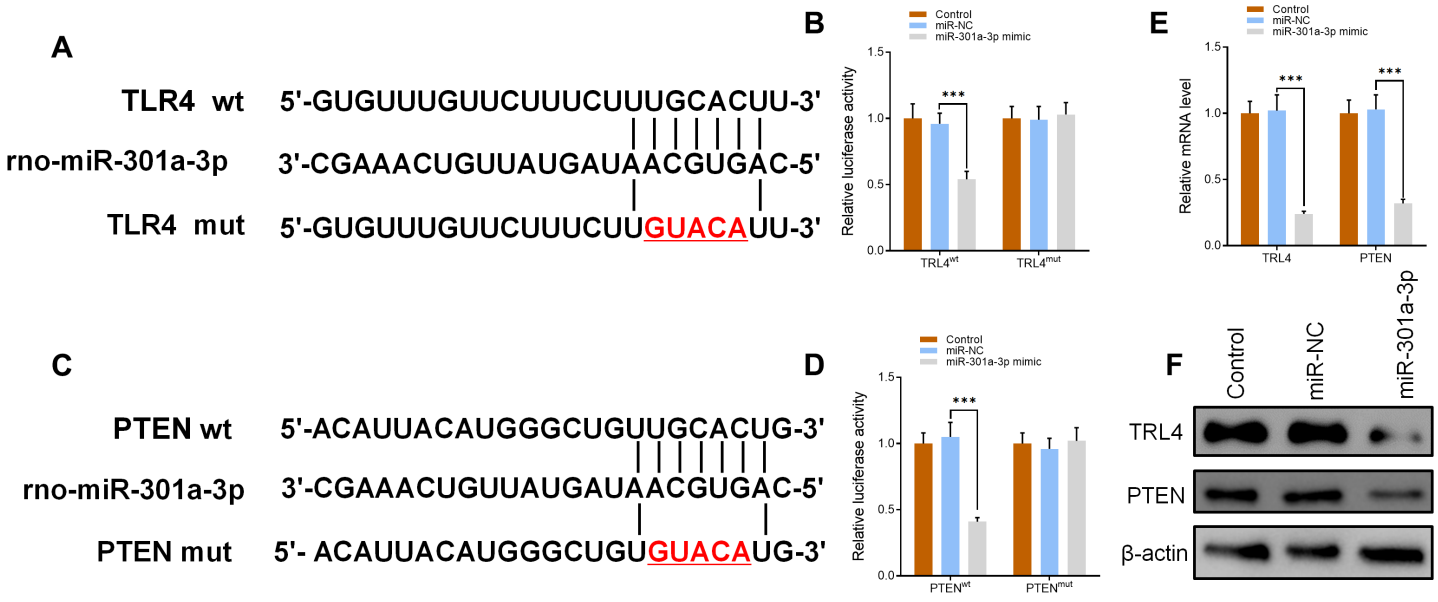

Figure 6

A) Protein levels of α-SMA in control, CIH, CIH+EXO, CIH+EXO-301a groups as measured by Western blotting. B and C) Flow cytometry results of apoptosis rate in all groups. D, E and F) Relative expression of miR-301a-3p, PTEN, and TLR4 level as determined by RT-qPCR. G and H) Protein levels of PTEN, TLR4,

HIF-1α, LC3I/II, p62 and p65 in CCSMCs as quantified by Western blotting. I, K, J and L) Results of mRFP-GFP-LC3 staining and quantitation of autophagosomes, autolysosomes, and autophagic vacuoles. Data are expressed as mean ± SD (n = 6; **p <0.01, ***p <0.001, ns mean none significant).

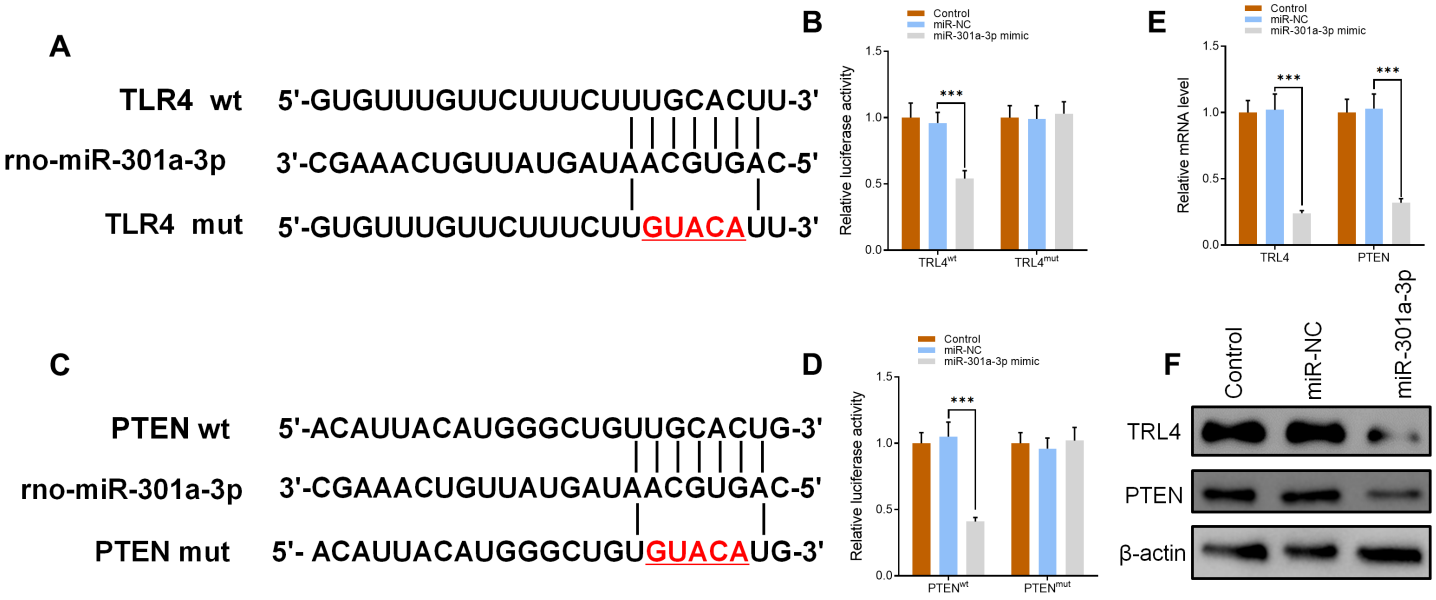

Figure 6

A) Protein levels of α-SMA in control, CIH, CIH+EXO, CIH+EXO-301a groups as measured by Western blotting. B and C) Flow cytometry results of apoptosis rate in all groups. D, E and F) Relative expression of miR-301a-3p, PTEN, and TLR4 level as determined by RT-qPCR. G and H) Protein levels of PTEN, TLR4, HIF-1α, LC3I/II, p62 and p65 in CCSMCs as quantified by Western blotting. I, K, J and L) Results of mRFP-GFP-LC3 staining and quantitation of autophagosomes, autolysosomes, and autophagic vacuoles. Data are expressed as mean ± SD (n = 6; **p <0.01, ***p <0.001, ns mean none significant).

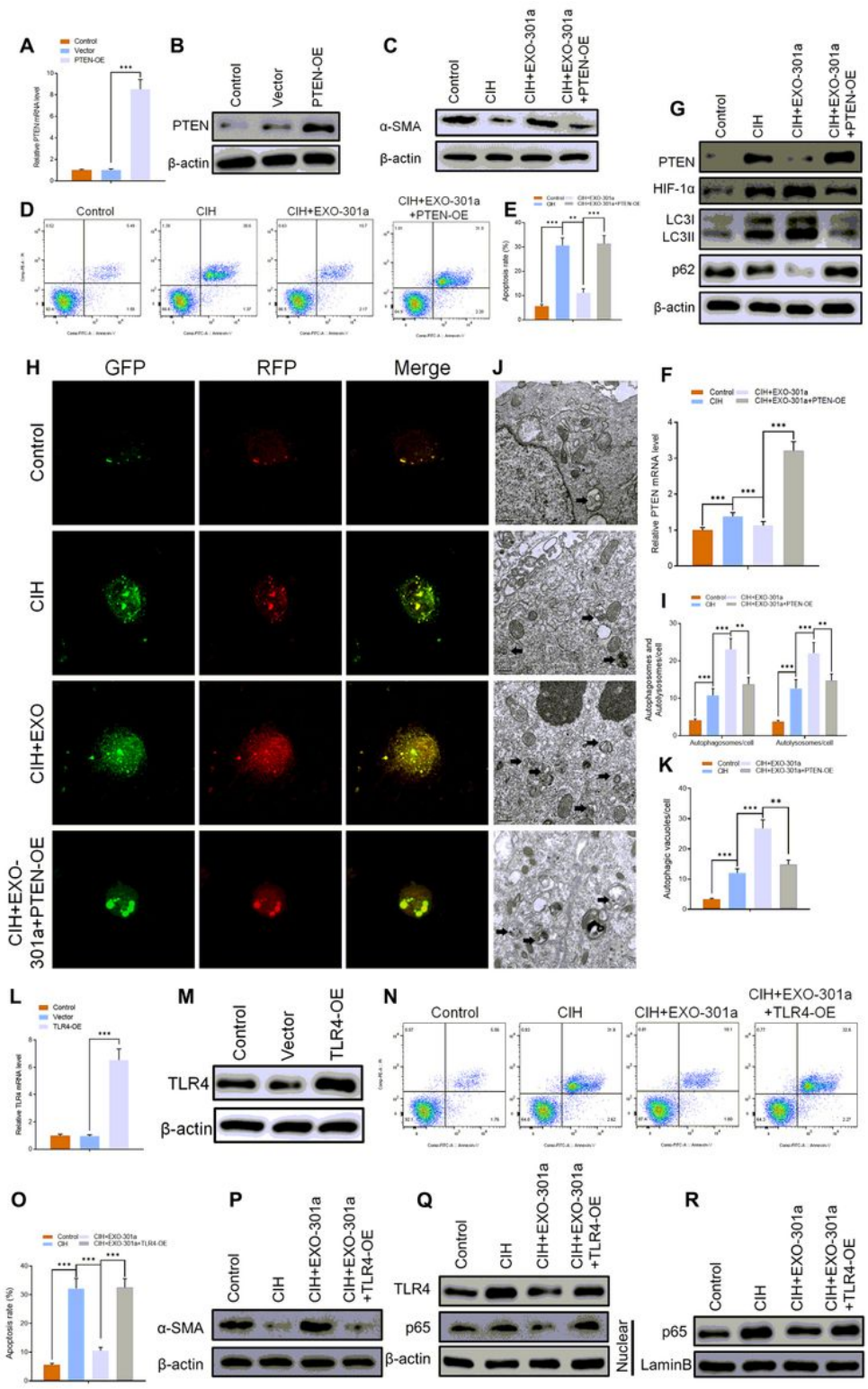

Figure 7

A and B) Relative mRNA and protein level of PTEN in control, vector, and PTEN-OE groups. C) Protein levels of α-SMA in control, CIH, CIH+EXO, CIH+EXO-301a groups as measured by Western blotting. D and E) Apoptosis rate in four groups as determined by Flow cytometry. F) RT-qPCR results of PTEN in four groups. (***p<0.001). G) Protein level of PTEN, HIF-1α, LC3I/II, p62 as assessed by Western blotting. H-K) mRFP-GFP-LC3 staining and quantitative results of autophagosomes, autolysosomes, and autophagic

vacuoles in the four groups. L and M) Relative mRNA and protein level of TLR4 in control, vector, and TLR4-OE groups. N and O) Level of apoptosis in control, CIH, CIH+EXO, CIH+EXO-301a groups. P-R) Protein levels of α-SMA, TLR4 and p65 as measured by Western blotting. Data are expressed as mean ± SD (n = 6; **p <0.01, ***p <0.001).

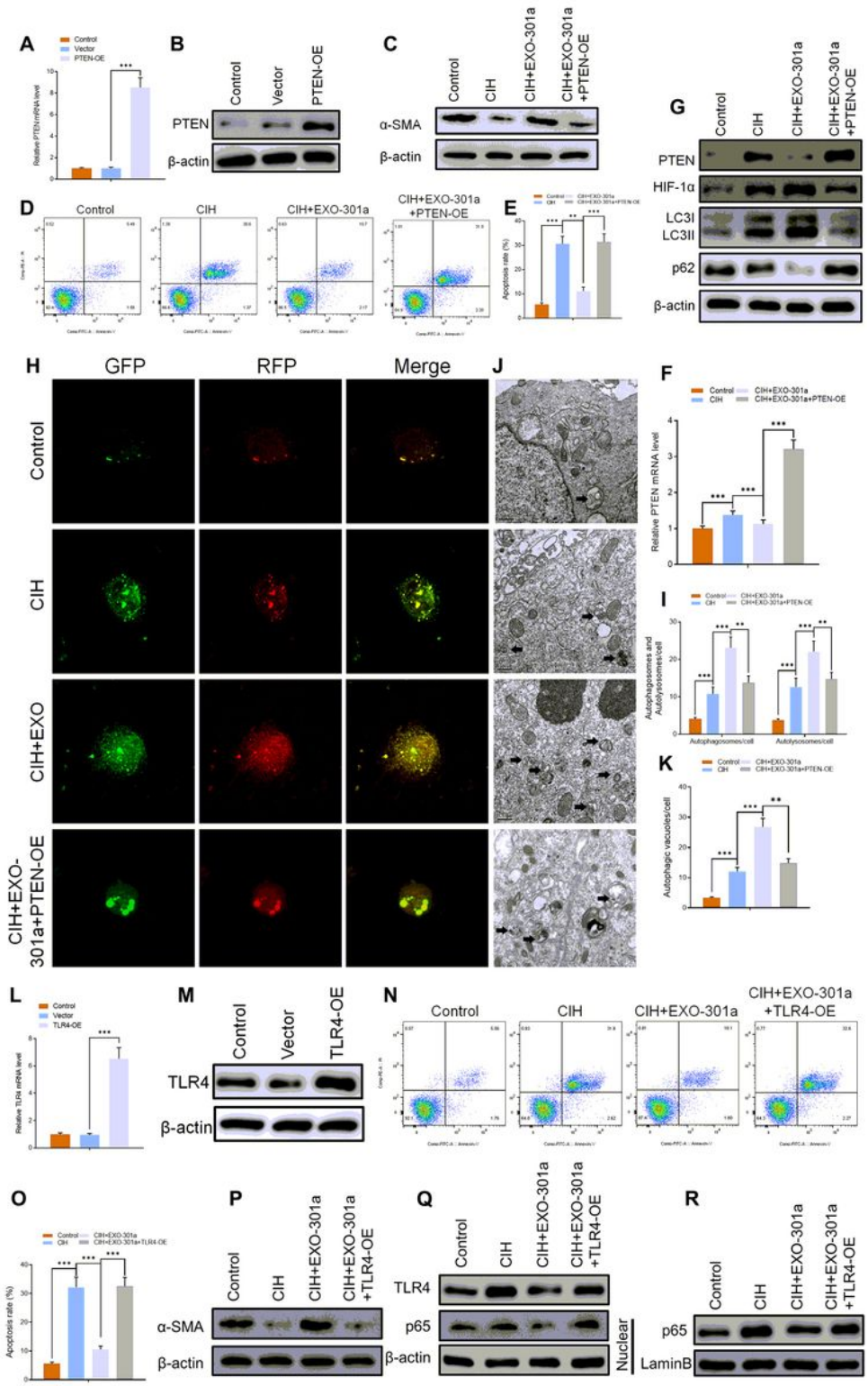

Figure 7

A and B) Relative mRNA and protein level of PTEN in control, vector, and PTEN-OE groups. C) Protein levels of α-SMA in control, CIH, CIH+EXO, CIH+EXO-301a groups as measured by Western blotting. D and E) Apoptosis rate in four groups as determined by Flow cytometry. F) RT-qPCR results of PTEN in four groups. (***p<0.001). G) Protein level of PTEN, HIF-1α, LC3I/II, p62 as assessed by Western blotting. H-K) mRFP-GFP-LC3 staining and quantitative results of autophagosomes, autolysosomes, and autophagic vacuoles in the four groups. L and M) Relative mRNA and protein level of TLR4 in control, vector, and TLR4-OE groups. N and O) Level of apoptosis in control, CIH, CIH+EXO, CIH+EXO-301a groups. P-R) Protein levels of α-SMA, TLR4 and p65 as measured by Western blotting. Data are expressed as mean ± SD (n = 6; **p <0.01, ***p <0.001).

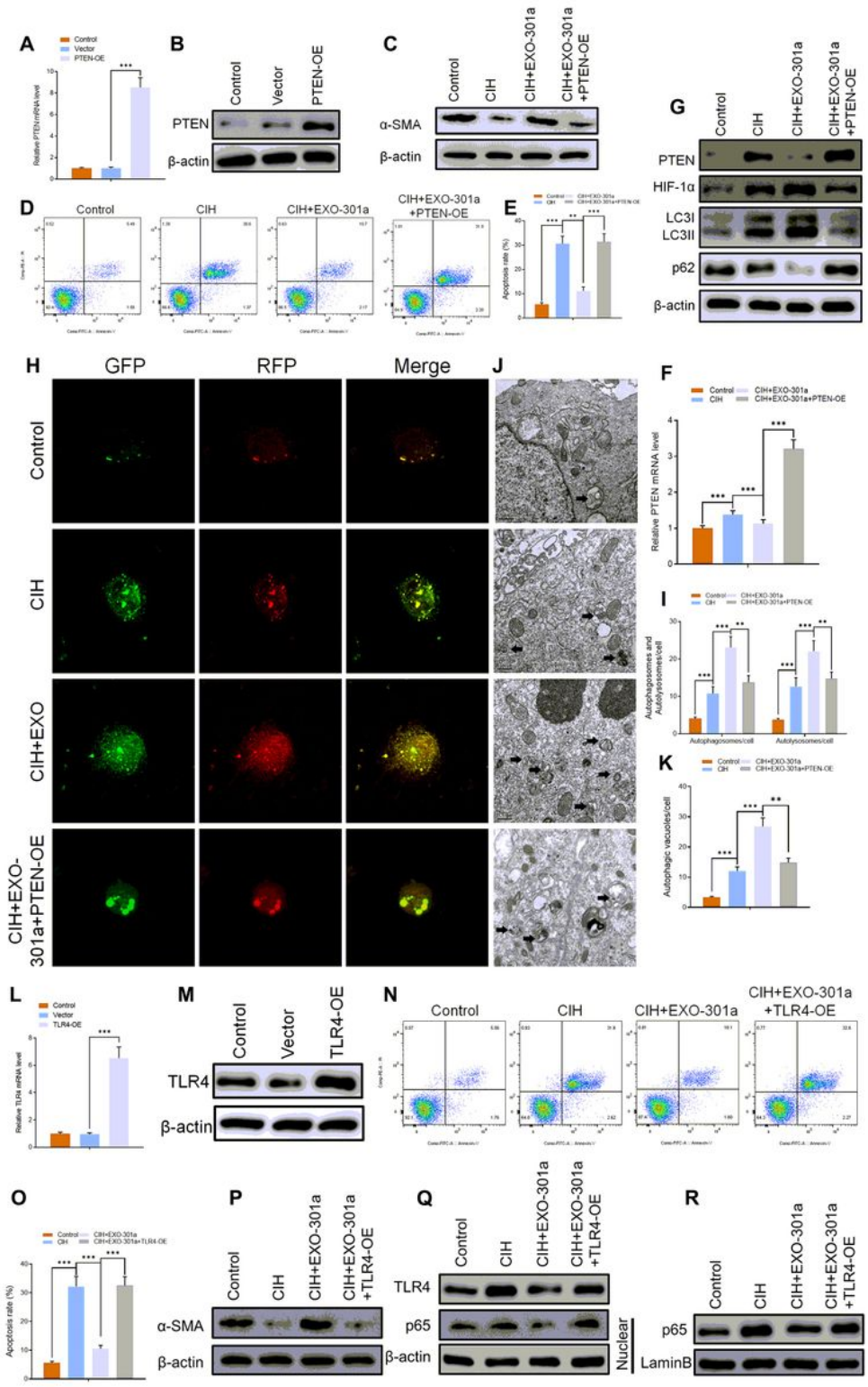

Figure 7

A and B) Relative mRNA and protein level of PTEN in control, vector, and PTEN-OE groups. C) Protein levels of α-SMA in control, CIH, CIH+EXO, CIH+EXO-301a groups as measured by Western blotting. D and E) Apoptosis rate in four groups as determined by Flow cytometry. F) RT-qPCR results of PTEN in four groups. (***p<0.001). G) Protein level of PTEN, HIF-1α, LC3I/II, p62 as assessed by Western blotting. H-K) mRFP-GFP-LC3 staining and quantitative results of autophagosomes, autolysosomes, and autophagic

vacuoles in the four groups. L and M) Relative mRNA and protein level of TLR4 in control, vector, and TLR4-OE groups. N and O) Level of apoptosis in control, CIH, CIH+EXO, CIH+EXO-301a groups. P-R) Protein levels of α-SMA, TLR4 and p65 as measured by Western blotting. Data are expressed as mean ± SD (n = 6; **p <0.01, ***p <0.001).

Supplementary Files

This is a list of supplementary files associated with this preprint. Click to download.

- SupplementaryMaterials.docx
- SupplementaryMaterials.docx
- SupplementaryMaterials.docx